

MIT Open Access Articles

*Spin liquids and pseudogap metals in the
SU(4) Hubbard model in a moiré superlattice*

The MIT Faculty has made this article openly available. **Please share**
how this access benefits you. Your story matters.

Citation: Zhang, Ya-Hui and Dan Mao. "Spin liquids and pseudogap metals in the SU(4) Hubbard model in a moiré superlattice." *Physical Review B* 101, 3 (January 2020): 035122 © 2020 American Physical Society

As Published: 10.1103/physrevb.101.035122

Publisher: American Physical Society (APS)


Persistent URL: <https://hdl.handle.net/1721.1/125590>

Version: Final published version: final published article, as it appeared in a journal, conference proceedings, or other formally published context

Terms of Use: Article is made available in accordance with the publisher's policy and may be subject to US copyright law. Please refer to the publisher's site for terms of use.



Spin liquids and pseudogap metals in the SU(4) Hubbard model in a moiré superlattice

Ya-Hui Zhang and Dan Mao *Department of Physics, Massachusetts Institute of Technology, Cambridge, Massachusetts 02139, USA*

(Received 9 July 2019; revised manuscript received 4 November 2019; published 13 January 2020)

Motivated by the realization of spin-valley Hubbard model on a triangular moiré superlattice in ABC trilayer graphene aligned with hexagonal boron nitride (hBN) and possibly also in twisted transition metal dichalcogenide homobilayers, we study possible Mott insulating phases and pseudogap metals based on symmetry constraint and parton mean field theories. First, we show that the Luttinger constraint allows two distinct symmetric and featureless Fermi liquids when there is an intervalley Hund's term breaking SU(4) spin rotation. Especially, there exists a symmetric and featureless “pseudogap metal” with small Fermi surfaces. Then, we suggest to search for such an unconventional metallic state by doping the Mott insulator at $\nu_T = 2$. For this purpose, we study the $\nu_T = 2$ Mott insulator using the SO(6) Schwinger boson or Schwinger fermion parton. At the SU(4)-symmetric point, we find two symmetric Z_2 spin liquids. With a large anti-intervalley Hund's term, a featureless Mott insulator is natural. Next, we show that doping the featureless Mott insulator or a Z_2 spin liquid can lead to featureless or orthogonal “pseudogap metal” with small Fermi surfaces proportional to the doping. Besides, we also provide one scenario for the evolution from pseudogap metal to the conventional Fermi liquid through an intermediate exotic “deconfined metal” phase. Last, we give brief comments on the possibility of U(1) spinon Fermi surface state or Z_4 spin liquid at $\nu_T = 1$.

DOI: [10.1103/PhysRevB.101.035122](https://doi.org/10.1103/PhysRevB.101.035122)

I. INTRODUCTION

Recently, moiré superlattices from Van der Waals heterostructures emerge to be a wonderful platform to study strongly correlated physics. These include correlated insulator [1], superconductivity [2–4], and anomalous Hall effect [5] in twisted bilayer graphene, spin-polarized correlated insulators [6–8], and superconductivity [6,7] in twisted bilayer-bilayer graphene. In addition, ABC trilayer graphene aligned with a hexagonal boron nitride (TLG-hBN) has been demonstrated to host gate-tunable correlated insulator [9], superconductor [10], and Chern insulator [11].

Theoretically, it has been shown that both bandwidth and band topology can be tuned by the displacement field in the TLG-hBN system [12,13]. For one sign of displacement field, the valence bands from the two valleys have nonzero and opposite Chern numbers. Similar narrow Chern bands have also been predicted in twisted bilayer graphene aligned with hBN [14,15] and in twisted bilayer-bilayer graphene [12,16–20]. These systems therefore may realize interesting “quantum Hall” physics. Indeed, anomalous Hall effect [5] and Chern insulator with $\sigma_{xy} = 2\frac{e^2}{h}$ [11] have already been reported. In contrast, for the other sign of displacement field in TLG-hBN, the valence band is trivial and there is no obstruction to build lattice models from constructing Wannier orbitals [21]. Such a spin-valley Hubbard model on triangular lattice is derived in Ref. [22]. $\frac{t}{V}$ in this Hubbard model can be tuned by the magnitude of the displacement field. Therefore, the trivial side of TLG-hBN offers an amazing platform to study Hubbard model physics [22–26], which may be similar to that of the cuprates. The observation of a superconductor in the trivial side [10] is encouraging. In cuprates, the pseudogap metal and the strange metal remain as an unsolved mystery in addition to the high- T_c superconductor. Then, a natural question is as

follows: Can TLG-hBN also host similar “pseudogap metal” and “strange metal” phases? In this paper, we try to give a positive answer to this question by explicitly constructing several simple pseudogap metal *Ansätze* in the spin-valley Hubbard model. A SU(4) Hubbard model on triangular lattice may also be realized in twisted transition metal dichalcogenide (TMD) homobilayer [27]. Therefore, our discussions can also be relevant to future experiments in twisted TMD bilayers.

In cuprates, a sensible theoretical scenario is that the strange metal is associated with a quantum critical point between the pseudogap metal and the conventional Fermi liquid (FL). However, the critical point, even if exists, is covered by the superconducting phase. When the superconductor is suppressed by strong magnetic field, in the underdoped region experiments observe signatures of small Fermi surfaces through quantum oscillation [28] and Hall measurement [29]. The area of the small Fermi pocket inferred from the experiment is proportional to the doped additional holes instead of all of the electrons. It is still under debate whether this high-field pseudogap metal is from some density wave orders [30,31] or is from a symmetric metal like fractionalized Fermi Liquid (FL*) phase [32,33]. As a matter of principle, density wave order parameter is not necessary to gap out Fermi surface and there should exist a symmetry pseudogap metal with small Fermi surfaces once fractionalization is allowed. However, we do not know any simple model so far to realize these symmetric metals with small Fermi surfaces. In this paper we will show that the spin-valley Hubbard model is very promising in this direction. More specifically, we show that at filling $\nu_T = 2 - x$, there are naturally symmetric pseudogap metals with Hall number $\eta_H = -x$. Depending on the value of intervalley Hund's coupling, the pseudogap metal is either a featureless Fermi liquid or an orthogonal metal [34].

We can understand the existence of pseudogap metals from two different perspectives. First, with an intervalley Hund's term, the U(4) symmetry is broken down to $[U(1) \times U(1)_{\text{valley}} \times SU(2)_{\text{spin}}]/Z_2$. Then, the Lieb-Schultz-Mattis (LSM) constraint allows two distinct symmetric and featureless Fermi liquids with Fermi-surface areas $A_{\text{FS}} = \frac{2-x}{4}$ or $A_{\text{FS}} = -\frac{x}{4}$. In the second perspective, symmetric pseudogap metals can be constructed from doping-symmetric Mott insulators. Therefore, we turn to study the possible symmetric Mott insulators at $\nu_T = 2$. Depending on the value of intervalley Hund's coupling J_H , we find a featureless insulator and two symmetric Z_2 spin liquids using SO(6) Schwinger boson or Schwinger fermion parton construction. Then, within a SO(6) slave-boson parton theory, doping the Mott insulator leads to a featureless Fermi liquid or an orthogonal metal. Both of them have small Fermi surfaces with area equal to $\frac{x}{4}$, resembling experimental results of underdoped cuprates under strong magnetic field. Compared to phenomenology in cuprates, the ansatz we propose here is much simpler: it is a ground state at zero magnetic field without breaking any symmetry. The simplicity of the proposed pseudogap metal may make it much easier to study its evolution toward the large Fermi-surface Fermi liquid and possible "strange metal" phase sandwiched in the intermediate region. We suggest one possible route through an intermediate "deconfined metal" with an internal U(1) gauge field. It remains a question whether a direct transition is possible or the property of the intermediate phase (or critical region) can mimic that of the strange metal in the cuprates.

In this paper, we focus on the limit that the anisotropic term breaking SU(4) spin rotation symmetry is small compared to the Heisenberg coupling. If the intervalley Hund's coupling is large, then the $\nu_T = 2$ Mott insulator has 120° Neel order [35] formed by spin-one moment. Physics from doping such a spin-one Neel order may also be interesting, but is beyond the scope of this paper.

Although, most of the paper is focused on filling close to $\nu_T = 2$. We also give a brief discussion on the Mott insulator at $\nu_T = 1$. At $\nu_T = 1$, we only find two symmetric spin liquids: a U(1) spinon Fermi-surface state or a Z_4 spin liquid. A plaquette order may be a strong competing candidate. With only nearest-neighbor coupling, magnetic order may be suppressed by strong quantum fluctuations. Therefore, we expect the $\nu_T = 1$ Mott insulator to preserve the approximation SU(4) spin rotation symmetry. Then, a charge- $4e$ superconductor may emerge from doping such a SU(4)-symmetric Mott insulator. It is interesting to study the possibility that the observed superconductor in TLG-hBN [10] is a charge- $4e$ paired state.

II. HAMILTONIAN AND SYMMETRY

A lattice model for TLG-hBN has been derived in Ref. [22]. To leading order it is a spin-valley model on triangular lattice:

$$H = -t \sum_a \sum_{\langle ij \rangle} e^{i\varphi_{ij}^a} c_{a,i}^\dagger c_{a,j} + \text{H.c.} + \frac{U}{2} n_i^2 + J_H \sum_i \mathbf{S}_{+i} \cdot \mathbf{S}_{-i}, \quad (1)$$

where $a = +, -$ is the valley index. We have suppressed the spin index. U is the Hubbard interaction and J_H is an onsite intervalley spin-spin coupling. $\varphi_{ij}^+ = -\varphi_{ij}^-$ provides the valley-contrasting staggered flux pattern.

At $\varphi_{ij}^a = 0$ and $J_H = 0$ limits, we have U(4) symmetry. Adding the valley-contrasting flux breaks the symmetry down to $U(2)_+ \times U(2)_-$, which is further broken down to $SU(2)_s \times U(1)_c \times U(1)_v/Z_2$ by the intervalley spin-spin coupling, where Z_2 stands for the common element of $SU(2)_s$, $U(1)_c$, and $U(1)_v$. The Coulomb interaction indicates that $J_H < 0$. However, electron phonon coupling from phonon at K and K' can mediate positive J_H [36]. The final sign of J_H is decided by the competition between these two effects. In this paper, we will view J_H as a phenomenological parameter to be fit from the experiment.

Next, we discuss the effective low-energy model in the $U \gg t$ limit with a restricted Hilbert space. $\nu_T \leq 2$ can be mapped to $\nu_T \geq 2$ by a particle-hole transformation and thus we only focus on $\nu_T \leq 2$.

A. Mott insulator

At integer $\nu_T = 1, 2$, the charge is localized and the low energy is described by an effective spin model. The dimension of the Hilbert space at each site is 4 and 6 ($6 = 4 \text{ choose } 2$), respectively, for $\nu_T = 1$ and 2. In the SU(4)-symmetric limit, we have

$$H_S = J \sum_{\langle ij \rangle} \sum_p S_i^p S_j^p \quad (2)$$

with $J = \frac{t^2}{2U} \cdot S_i^p$, with $p = 1, 2, \dots, 15$, is a spin operator on each site. These 15 spin operators can be organized as $S^{\mu\nu} = \tau^\mu \sigma^\nu$ with $\mu, \nu = 0, 1, 2, 3$ except $\mu = \nu = 0$. Each of them is a fermion bilinear:

$$S_i^{\mu\nu} = \sum_{a_1, a_2} \sum_{\sigma_1 \sigma_2} c_{a_1 \sigma_1 i}^\dagger \tau_{a_1 a_2}^\mu \sigma_{\sigma_1 \sigma_2}^\nu c_{a_2 \sigma_2 i}. \quad (3)$$

Projecting to the four- and six-dimensional Hilbert space at each site for $\nu_T = 1, 2$, $S^{\mu\nu} = \tau^\mu \sigma^\nu$ should be viewed as 4×4 and 6×6 matrices for $\nu_T = 1$ and 2.

The spin Hamiltonian has $\text{PSU}(4) = \text{SU}(4)/Z_4$ symmetry. Here, Z_4 means the global U(1) transformation $e^{i\frac{2\pi}{4}n}$ with n as an integer. At $\nu_T = 2$, each site is in the $6d$ -irrep of SU(4), which transforms like SO(6) fundamental under SU(4) [$\text{SO}(6) \cong \text{SU}(4)/Z_2$].

For the TLG-hBN system, there is a valley-contrasting phase in the hopping term [22]. Two valleys have opposite staggered flux patterns. This valley-dependent flux on the hopping term is inherited in the t^2/U expansion and gives an anisotropy term

$$H_S^i = J \sum_{\langle ij \rangle} (\cos 2\varphi_{ij} - 1) (\tau_i^x \tau_j^x + \tau_i^y \tau_j^y) (1 + \vec{\sigma}_i \cdot \vec{\sigma}_j) + J \sum_{\langle ij \rangle} \sin 2\varphi_{ij} (\tau_i^x \tau_j^y - \tau_i^y \tau_j^x) (1 + \vec{\sigma}_i \cdot \vec{\sigma}_j), \quad (4)$$

where φ_{ij} is the phase in the hopping for the valley $+$ on bond $\langle ij \rangle$ (correspondingly, the valley $-$ has phase $-\varphi_{ij}$ for the hopping on the same bond).

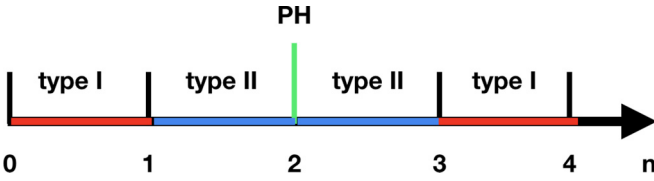


FIG. 1. Two distinct t - J models in four-flavor spin-valley Hubbard model. $\nu_T < 2$ and $\nu_T > 2$ are related by particle-hole transformation. $\nu_T < 1$ and $1 < \nu_T < 2$ realize two essentially different t - J models.

The above symmetry breaks the PSU(4) spin rotation down to $\text{SO}(3)_+ \times \text{SO}(3)_- \times \text{U}(1)_v$. For $\nu_T = 2$ the corresponding spin rotation symmetry can be viewed as $\text{U}(1)_v \times \text{SO}(4)/\mathbb{Z}_2 \cong \text{SO}(3)_+ \times \text{SO}(3)_- \times \text{U}(1)_v$, where SO(4) acts on the $4d$ space formed by three valley singlet, spin triplet and one valley triplet, spin singlet.

For $\nu_T = 2$, there is an additional onsite intervalley spin-spin coupling:

$$H_S'' = J_H \sum_i \vec{S}_i^+ \cdot \vec{S}_i^- \quad (5)$$

We define the valley-specified spin operator

$$\vec{S}_i^a = \frac{1}{2} \sum_{\sigma_1, \sigma_2 = \uparrow, \downarrow} c_{i;a;\sigma_1}^\dagger \vec{\sigma}_{\sigma_1 \sigma_2} c_{i;a;\sigma_2} \quad (6)$$

for $a = +, -$. H_S'' vanishes for $\nu_T = 1$. For $\nu_T = 2$, it further breaks the spin rotation symmetry down to $\text{U}(1)_{\text{valley}} \times \text{SO}(3)_{\text{spin}}$.

B. Finite doping: Type I and II t - J models

In spin- $\frac{1}{2}$ Hubbard model, the physics at finite doping away from the Mott insulator is believed to be governed by a t - J model at the $U \gg t$ limit. Here we want to show that for the spin-valley Hubbard model, the region $1 < \nu_T < 2$ has different physics from the traditional t - J model in the region $0 < \nu_T < 1$. Therefore, the four-flavor Hubbard model can actually realize two distinct t - J models, which is illustrated in Fig. 1.

1. $\nu_T = 1 - x$: Type I t - J model

At filling $\nu_T = 1 - x$ with $0 < x < 1$, the low energy is described by a similar t - J model as in the spin- $\frac{1}{2}$ case:

$$H = -t \sum_{\langle ij \rangle} P_i c_i^\dagger c_j P_i + J \sum_{\langle ij \rangle} S_i^p S_j^p + H_S', \quad (7)$$

where P_i is the projection operator which forbids states with $n \geq 2$ on each site.

For $\nu_T = 1 - x$, the onsite intervalley spin-spin coupling J_H term vanishes in the leading order of t/U because of the restriction of the Hilbert space. It enters in the second order of t/U by changing the spin coupling from $\frac{t^2}{U}$ to $\frac{t^2}{U \pm J_H}$. The change of the spin coupling is $\delta J \sim \frac{J_H}{U} J \ll J$ and can be ignored given the estimation that $J_H \sim 0.01U$ [22]. Therefore, there is an approximating $\text{U}(2)_+ \times \text{U}(2)_-$ symmetry at the $U \gg t$ limit even if $J_H \neq 0$.

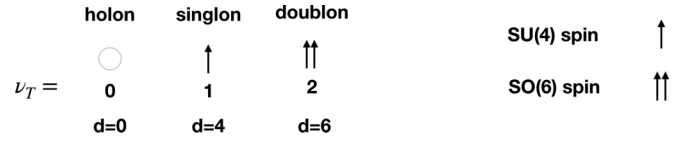


FIG. 2. Label of several different states according to the number of particle n_i at the site. Holon is an empty site. Singlon and doublon are in the fundamental rep and the SO(6) rep of the SU(4) group, respectively. The Hilbert space dimensions of the holon, singlon, doublon states are 1, 3, and 6, respectively.

In this type I t - J model, each site is either empty or singly occupied, similar to that of hole-doped cuprate [37]. For convenience, in this paper we call the empty site as holon and the singly occupied site as singlon (see Fig. 2). The Hilbert space dimension of each site is $1 + 4 = 5$. The t - J model has unusual property that the singlon density is conserved to be $1 - x$ while the holon density is conserved to be x . The t term in Eq. (7) is not a traditional hopping term. Instead, it involves the exchange between a holon at site i with a singlon at site j .

2. $\nu_T = 2 - x$: Type II t - J model

At filling $\nu_T = 2 - x$ with $0 < x < 1$, we have either a singlon or a doublon state at each site in the $U \gg t$ limit. Thus, the Hilbert space dimension at each site is $4 + 6 = 10$. In addition, the singlon and the doublon carry different representations of SU(4) spin. Hence, there are three different spin couplings (see Fig. 3). We define P_s and P_d as the projection operators to the singlon and the doublon states, respectively. Then, it is natural to have spin operators for the singlon and doublon: $S_{i;s}^{\mu\nu} = P_s S_i^{\mu\nu} P_s$ and $S_{i;d}^{\mu\nu} = P_d S_i^{\mu\nu} P_d$. We have the type II t - J model as

$$H = -t \sum_{\langle ij \rangle} (P_s + P_d) c_i^\dagger c_j (P_s + P_d) + J \sum_{\langle ij \rangle} S_{i;s}^p S_{j;s}^p + \frac{1}{2} J' \sum_{\langle ij \rangle} (S_{i;s}^p S_{j;d}^p + S_{i;d}^p S_{j;s}^p) + J_d \sum_{\langle ij \rangle} S_{i;d}^p S_{j;d}^p + H_S' + H_S'', \quad (8)$$

where $J' = \frac{1}{2}J$ and $J_d = J$. In the superexchange process involving a singlon and a doublon nearby, the only process

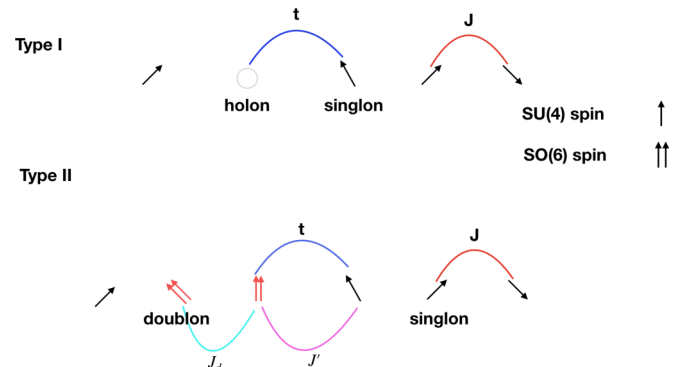


FIG. 3. Illustration of the type I and II t - J models. In type II model, there are three different spin-spin couplings.

we should keep is to hop the particle from the singlon to the doublon, which costs energy $2U$ instead of U . This is how the two factors $\frac{1}{2}$ arise. Because of the H_S'' term, generically we only have $U(2) \times U(1)_{\text{valley}}$ spin rotation symmetry.

The two t - J models in Eqs. (7) and (8) are apparently quite different. In the type II t - J model, there is no empty site in the Hilbert space. Instead, the singlon and doublon both carry spin. The kinetic term now becomes the exchange of the singlon and doublon. Recently, a similar type II t - J model has been proposed [38] to describe the nickelate superconductor [39]. There there is only $SU(2)$ spin rotation symmetry and the singlon and doublon carry $S = \frac{1}{2}$ and 1, respectively. This t - J model can be derived from the $SU(4)$ -symmetric t - J model in this paper by adding anisotropic terms. Therefore, our analysis in this paper may also provide insights to the solid-state realization of type II t - J model using the two e_g orbitals.

In the familiar t - J model, at least for large doping, the most natural ground state is a conventional Fermi liquid. This state can be constructed within the simple slave-boson mean field theory [37] which respects the constraint P_1 . The simple way to understand this Fermi-liquid state is that the holons condense and the singlons form Fermi surfaces. This picture can be easily generalized to the case $\nu_T = 1 - x$ for the spin-valley Hubbard model. However, for $\nu_T = 2 - x$, neither the singlons nor the doublons can form Fermi surfaces whose areas match a conventional Fermi liquid. In this case, description of a conventional Fermi liquid is very hard if we insist to respect the constraint $P_s + P_d$. As we show later, a generalized slave-boson mean field theory naturally predicts pseudogap metals with Fermi-surface areas proportional to x instead of ν_T . We can still describe a conventional Fermi-liquid phase, but it requires a more exotic parton construction if we want to respect the constraint P_2 .

III. SYMMETRY CONSTRAINT: LUTTINGER THEOREM

Before we move to discussions of specific fillings, we give a general symmetry analysis in this section. We will consider LSM type of constraints based on the simple Oshikawa-flux threading argument [40]. The argument and the constraint works for both integer and incommensurate filling. Besides, the symmetry analysis in this section is independent of models and also applies to the case with topological bands.

The symmetries that we consider here are translation, spin rotation, charge conservation, and time reversal. Depending on whether we include the intervalley spin-spin coupling, we consider $U(2)_+ \times U(2)_-$ spin rotation symmetry and $U(1)_c \times U(1)_v \times SO(3)_s$ separately. In all cases we assume there is a time-reversal symmetry which exchanges the two valleys.

A. Symmetry $U(4)$ or $U(2)_+ \times U(2)_-$

The constraint is the same for $U(4)$ and $U(2)_+ \times U(2)_-$. For simplicity, we will only use $U(2)_+ \times U(2)_-$. Note that time reversal exchanges two valleys so the density for each flavor is guaranteed to be $\nu = \frac{\nu_T}{4}$. Meanwhile, we have $U(1)^4 \subset U(2)_+ \times U(2)_-$, which means we have $U(1)$ symmetry for each flavor. Then, we can do flux insertion for one valley-spin species out of four. Using Oshikawa's argument [40], one can

reach the conclusion that any symmetric and featureless phase needs to have Fermi-surface area $A_{\text{FS}} = \nu \text{ mod } n = \frac{\nu_T}{4} \text{ mod } n$, where n is an integer.

For $\nu_T = 1, 2$, the above constraint means there must be a Fermi surface with area $\frac{1}{4}$ or $\frac{1}{2}$ for each flavor. Therefore, a symmetric and featureless Mott insulator is not possible for symmetry $U(2)_+ \times U(2)_-$.

B. Symmetry $[U(1)_c \times U(1)_v \times SU(2)_s]/Z_2$: Two distinct symmetric and featureless states

When there is a nonzero J_H , the global symmetry is $[U(1)_c \times U(1)_v \times SU(2)_s]/Z_2$. There is no separate spin rotation symmetry for each valley. Only the total spin rotation is conserved in this case. There are only three independent $U(1)$ global symmetries (corresponding to N , S_z , and τ_z) that belong to $[U(1)_c \times U(1)_v \times SU(2)_s]/Z_2$. [Recall that there are four $U(1)$ charges in the previous subsection.] Gauging these three $U(1)$ symmetries yields three independent flux insertions. We cannot do flux insertion for each valley-spin species. The best we can do is to include at least two valley-spin species in the flux insertion process in order to respect the global symmetry. Since we still have time-reversal and total spin rotation symmetry, the filling per valley per spin is still fixed to be $\nu = \frac{\nu_T}{4}$, ν_T being the total filling. If the ground state is a symmetric Fermi liquid, the Fermi-surface area for every flavor must be equal to each other. Let us perform an adiabatic $U(1)$ flux insertion for both spins of the $+$ valley. The constraint one can get using Oshikawa's argument is $A_{\text{FS},+\uparrow} + A_{\text{FS},+\downarrow} = 2A_{\text{FS}} = \nu_{+\uparrow} + \nu_{+\downarrow} (\text{mod } n) = \frac{\nu_T}{2} (\text{mod } n)$, where n is an integer. This yields $A_{\text{FS}} = \frac{\nu_T}{4} (\text{mod } m)$ or $A_{\text{FS}} = (\frac{\nu_T}{4} - \frac{1}{2}) (\text{mod } m)$, where m is an integer.

Interestingly, we find that there are two distinct symmetric and featureless Fermi liquids. One of them is connected to the free-fermion model while the other one has smaller Fermi surfaces and may be viewed as a "pseudogap metal." The essential point of the argument is that there are only three $U(1)$ charges while there are four flavors. Meanwhile, the symmetry is sufficient to forbid bilinear term with interflavor coupling and guarantee four equal Fermi surfaces. The above two conditions can not be satisfied simultaneously in the traditional spin- $\frac{1}{2}$ system. This is a special feature of spin-valley model realized in moiré superlattices.

At $\nu_T = 2$, we are allowed to have $A_{\text{FS}} = \frac{1}{2}$ or $A_{\text{FS}} = 0$, which implies the existence of a symmetric and featureless Mott insulator. We need to emphasize that $U(1)_v$ and time-reversal symmetry is important to guarantee the existence of the two distinct classes. Without time reversal, we can have a "band insulator" at $\nu_T = 2$ by polarizing valley. This band insulator can smoothly connect to the conventional Fermi liquid by reducing the τ_z polarization. Once we have time-reversal symmetry, the density of each flavor is fixed to be $\frac{1}{2}$ at $\nu_T = 2$. In this case, the featureless Mott insulator can not smoothly cross over to the conventional Fermi liquid and can not be described by mean field theory with any order parameter.

We will construct both the featureless insulator at $\nu_T = 2$ and the featureless pseudogap metal in Secs. V and VII for the spin-valley Hubbard model. The essential physics behind

them is *singlet formation*. At $\nu_T = 2$, there are N electrons in the valley $+$ and N electrons in the valley $-$, where N is the number of moiré unit cells. These electrons can be gapped out by forming intervalley singlets. If we further dope electrons or holes with density x , these additional doped carriers just form small Fermi surfaces with area $A_{\text{FS}} = \frac{x}{4}$ on top of the featureless Mott insulator.

Although the picture of the featureless insulator and the featureless pseudogap metal is very simple, they can not be described by the conventional mean field theory with symmetry-breaking order parameters. In the cuprate context, symmetric pseudogap metals with small Fermi surfaces have been proposed before [32,33]. In the so called FL* phase, additional holes form small Fermi surfaces on top of a Z_2 spin liquid. The physics behind is still singlet formation: N number of electrons form resonating valence bond (RVB) singlets and the additional holes move on top of the RVB singlets. The difference in our case is that we can have onsite intervalley singlets and do not need to invoke fractionalization. In this sense, the featureless pseudogap metal we propose here is the simplest version of a symmetric pseudogap metal.

This simple symmetric pseudogap metal is beyond any conventional mean field theories with symmetry breaking because the singlet formation does not break any symmetry. So, how do we describe the singlet formation? It turns out that the singlet formation can be captured in a simple six-flavor slave-boson parton mean field theory. We will introduce the parton construction for the $\nu_T = 2$ Mott insulator first and then generalize it to the doped case to describe the featureless pseudogap metal. This slave-boson parton also allows us to describe another orthogonal pseudogap metal in the SU(4)-symmetric limit.

IV. PROJECTIVE SYMMETRY GROUP ANALYSIS

AT $\nu_T = 2$

A. Hilbert space

At $\nu_T = 2$, the Hilbert space is six dimensional at each site. There are six bases: $|\alpha\rangle = \sum_{ab} A_{ab}^\alpha c_a^\dagger c_b^\dagger |0\rangle$ with $\alpha = 1, 2, 3, 4, 5, 6$. A^α is a 4×4 antisymmetric matrix. We define the SU(4) flavor as $1 : +\uparrow, 2 : +\downarrow, 3 : -\uparrow, 4 : -\downarrow$. Each basis α is created by an operator Ψ_α^\dagger . We can define the following six bases:

$$\begin{aligned}
 \psi_1 &= \frac{1}{2\sqrt{2}} c^T \tau_z \sigma_y c = \frac{i}{\sqrt{2}} (-\Phi_{12} + \Phi_{34}), \\
 \psi_2 &= \frac{1}{2\sqrt{2}} c^T i \sigma_y c = \frac{1}{\sqrt{2}} (\Phi_{12} + \Phi_{34}), \\
 \psi_3 &= \frac{1}{2\sqrt{2}} c^T \tau_x \sigma_y c = \frac{i}{\sqrt{2}} (-\Phi_{14} + \Phi_{23}), \\
 \psi_4 &= \frac{1}{2\sqrt{2}} c^T i \tau_y \sigma_x c = \frac{1}{\sqrt{2}} (\Phi_{14} + \Phi_{23}), \\
 \psi_5 &= \frac{1}{2\sqrt{2}} c^T i \tau_y \sigma_z c = \frac{1}{\sqrt{2}} (\Phi_{13} - \Phi_{24}), \\
 \psi_6 &= \frac{1}{2\sqrt{2}} c^T \tau_y c = -\frac{i}{\sqrt{2}} (\Phi_{13} + \Phi_{24}), \tag{9}
 \end{aligned}$$

TABLE I. The correspondence between the generator of the SO(6) and the generators of the SU(4). For example, the SU(4) transformation $U = e^{i\tau_z \frac{\theta}{2}}$ corresponds to a rotation between ψ_1 and ψ_2 with angle θ .

τ_x	τ_y	τ_z	σ_x	σ_y	σ_z	$\tau_x \sigma_x$	$\tau_x \sigma_y$	$\tau_x \sigma_z$	$\tau_y \sigma_x$	$\tau_y \sigma_y$	$\tau_y \sigma_z$	$\tau_z \sigma_x$	$\tau_z \sigma_y$	$\tau_z \sigma_z$
S_{32}	S_{31}	S_{12}	S_{64}	S_{45}	S_{65}	S_{15}	S_{16}	S_{41}	S_{52}	S_{62}	S_{24}	S_{53}	S_{63}	S_{34}

where $\Phi_{ab} = \frac{1}{2}(c_a c_b - c_b c_a)$. These six states are organized to have clear physical meaning: the first three are valley triplet and spin singlet, while the latter three are valley singlet and spin triplet.

Let us define $\Psi^T = (\psi_1, \psi_2, \psi_3, \psi_4, \psi_5, \psi_6)$. It can be proved that the transformation is $\Psi' = O\Psi$ under the microscopic SU(4) transformation. O is a SO(6) matrix. There are 15 generators for the SO(6). We list them in Table I. The physical spin operator $S^{\mu\nu}$ defined in Eq. (3) can be written as a 6×6 matrix in the above basis. It is convenient to express it as $S^{\mu\nu} = \Psi^\dagger A^{\mu\nu} \Psi$. It turns out that the 6×6 matrix $A^{\mu\nu}$ only has two nonzero matrix elements. More specifically, each spin operator $S^{\mu\nu}$ corresponds to a (α, β) pair as listed in Table I. Then, $S^{\mu\nu} = S^{\alpha\beta} = 2i(\psi_\alpha^\dagger \psi_\beta - \psi_\beta^\dagger \psi_\alpha)$. For example, $\tau^x = 2i(\psi_3^\dagger \psi_2 - \psi_2^\dagger \psi_3)$.

When $H_S'' = H_S' = 0$, the spin model has SO(6)/ Z_2 symmetry where Z_2 consists of the 6×6 matrix $-I$. When $H_S' \neq 0$, the spin rotation symmetry is [SO(2) \times SO(4)]/ Z_2 . The Hilbert space at each site is decomposed to $6 = 2 \oplus 4$. (ψ_1, ψ_2) transforms as SO(2) corresponding to U(1)_{valley}. $(\psi_3, \psi_4, \psi_5, \psi_6)$ transforms as SO(4) under SU(2)₊ \times SU(2)₋. If we further add the onsite intervalley spin coupling H_S'' , the spin rotation symmetry is further reduced to SO(2) \times SO(3). The Hilbert space at each site is decomposed to three irreducible representations: $6 = 1 \oplus 2 \oplus 3$. ψ_3 forms a trivial representation. (ψ_1, ψ_2) transforms under SO(2), and (ψ_4, ψ_5, ψ_6) transforms under SO(3) in the same way as a spin-one degree of freedom.

For spin rotation symmetry SO(6)/ Z_2 and [SO(2) \times SO(4)]/ Z_2 , there is no symmetric gapped state. For the symmetry SO(2) \times SO(3), a featureless insulator is possible. For example, the state $\prod_i \psi_3^\dagger(i) |0\rangle$ is a featureless Mott insulator. However, we need a large $J_H > 0$ to favor this featureless insulating phase. In the trilayer graphene/hBN system, we expect $|J_H|$ to be smaller or at most comparable with J . When $J \gg |J_H|$, other phases including magnetic order, valence bond solid (VBS), and spin liquids may be favored. In this paper we try to classify all of possible symmetry spin-liquid phases based on the projective symmetric group (PSG) analysis.

B. Parton theories at $\nu_T = 2$

For $\nu_T = 2$, there are three different parton theories which we introduce in this section.

1. Abrikosov fermion

The first parton theory is the Abrikosov fermion parton which has been widely used in the treatment of spin- $\frac{1}{2}$ systems. We introduce fermionic operator $f_{i;a}$ with $a = 1, 2, 3, 4$.

The constraint is $\sum_a f_{i;a}^\dagger f_{i;a} = 2$. There is a U(1) gauge structure. As we will discuss later, the only symmetric spin liquid from the Abrikosov fermion parton is U(1) spin liquid with four Fermi surfaces, each at filling $\frac{1}{2}$.

2. Six-flavor Schwinger boson

Because the Hilbert space at each site is six dimensional and forms the fundamental representation of SO(6), we can use a six-flavor Schwinger boson parton construction. Basically, we identify Ψ_α in Eq. (9) as a bosonic operator b_α , where $\alpha = 1, 2, \dots, 6$. Correspondingly, the spin operator $S^{\alpha\beta} = 2i(b_\alpha^\dagger b_\beta - b_\beta^\dagger b_\alpha)$. For simplicity, we define a six-dimensional spinor $B(\mathbf{r}) = (b_1(\mathbf{r}), b_2(\mathbf{r}), b_3(\mathbf{r}), b_4(\mathbf{r}), b_5(\mathbf{r}), b_6(\mathbf{r}))$. The constraint is $B^\dagger(\mathbf{r})B(\mathbf{r}) = 1$ for each site \mathbf{r} . The gauge structure is U(1).

We define hopping term $\hat{T}_{ij} = B_i^\dagger B_j$ and $\hat{\Delta}_{ij} = \frac{1}{\sqrt{2}}(B_i^\dagger B_j + B_j^\dagger B_i)$. $\hat{T}_{ij}^\dagger = T_{ji}$. $\hat{\Delta}_{ij}^\dagger = \frac{1}{\sqrt{2}}(B_j^\dagger B_i^{\dagger T} + B_i^\dagger B_j^{\dagger T})$. Apparently, $\hat{\Delta}_{ij} = \hat{\Delta}_{ji}$.

The Hamiltonian in the SO(6) invariant limit can be written as

$$H = 4J \sum_{\langle ij \rangle} \hat{T}_{ij} \hat{T}_{ji} - 4J \sum_{\langle ij \rangle} \hat{\Delta}_{ij}^\dagger \hat{\Delta}_{ij}. \quad (10)$$

In the Schwinger boson theory, a typical mean field *Ansatz* is

$$H_M = \sum_{\langle ij \rangle} (T_{ij} \hat{T}_{ij} + \Delta_{ij}^\dagger \hat{\Delta}_{ij}), \quad (11)$$

where T_{ij} and Δ_{ij} are mean field parameters. For Schwinger boson, the meaningful *Ansatz* has $\Delta_{ij} \neq 0$, which describes a Z_2 spin liquid.

3. Six-flavor Schwinger fermion

Similar to the six-flavor Schwinger boson approach, we can also identify each basis $|\alpha\rangle$ in Eq. (9) to be created by a fermionic operator Ψ_α . Defining $\Psi = (\Psi_1, \Psi_2, \Psi_3, \Psi_4, \Psi_5, \Psi_6)$. The constraint is $\Psi^\dagger(\mathbf{r})\Psi(\mathbf{r}) = 1$ for each site \mathbf{r} . The gauge structure is $O(2) = Z_2 \times U(1)$. Z_2 corresponds to a charge conjugation $C: \Psi(\mathbf{r}) \rightarrow \Psi^\dagger(\mathbf{r})$. We define hopping term $\hat{T}_{ij} = \Psi_i^\dagger \Psi_j$ and $\hat{\Delta}_{ij} = \frac{1}{2}(\Psi_i \Psi_j - \Psi_j \Psi_i)$. $\hat{T}_{ij}^\dagger = \hat{T}_{ji}$. $\hat{\Delta}_{ij}^\dagger = \frac{1}{2}(\Psi_j^\dagger \Psi_i^\dagger - \Psi_i^\dagger \Psi_j^\dagger)$. Apparently, $\hat{\Delta}_{ij} = -\hat{\Delta}_{ji}$.

The SO(6) invariant Hamiltonian can be written as

$$H = -4J \sum_{\langle ij \rangle} \hat{T}_{ij} \hat{T}_{ji} - 4J \sum_{\langle ij \rangle} \hat{\Delta}_{ij}^\dagger \hat{\Delta}_{ij}. \quad (12)$$

The typical mean field *Ansatz* in the Schwinger fermion approach is

$$H_M = \sum_{\langle ij \rangle} (T_{ij} \hat{T}_{ij} + \Delta_{ij}^\dagger \hat{\Delta}_{ij}), \quad (13)$$

where T_{ij} and Δ_{ij} are mean field parameters. For Schwinger fermion parton theory, we can have both U(1) spin liquid with $\Delta_{ij} = 0$ and Z_2 spin liquid with $\Delta_{ij} \neq 0$. If Δ_{ij} is chiral, we can also have chiral spin liquid.

C. PSG classification of U(1) spin liquids at $\nu_T = 2$

We first discuss the U(1) spin liquid. There are two different kinds of U(1) spin-liquid phases. One is constructed from the Abrikosov fermion and the other one is constructed from the Schwinger fermion. For both Abrikosov fermion and Schwinger fermion, symmetry U(1) spin liquids have the same classification as shown in Appendix B. Both zero-flux phase and π -flux phase are symmetric. However, nearest-neighbor and next-nearest-neighbor hoppings in the π -flux phase are forbidden by the PSG, which is not physical. Therefore, we only consider the zero-flux phase for both the Abrikosov fermion parton and the Schwinger fermion parton.

From the Abrikosov fermion, we have a U(1) spin liquid with four Fermi surfaces, each of which is at filling $\frac{1}{2}$. This spin-liquid phase can go through a continuous transition to Fermi liquid. Basically, one can write the electron operator as $c_{i;a} = e^{i\theta_i} f_{i;a}$ and let the bosonic rotor go through a continuous superfluid-Mott transition [41].

From the Schwinger fermion, we have a U(1) spin liquid with six Fermi surfaces, each of which is at filling $\frac{1}{6}$. This U(1) spinon Fermi-surface phase is not connected to the Fermi liquid through direct transition.

D. PSG classification of Z_2 spin liquids at $\nu_T = 2$

We then classify symmetric Z_2 spin liquids at $\nu_T = 2$. The Z_2 spin liquid can be constructed from both the Schwinger boson parton and the Schwinger fermion parton. The PSG is the same for both Schwinger boson and Schwinger fermion parton constructions. It is independent of the spin rotation symmetry and therefore is true even if the SO(6)/ Z_2 spin rotation is broken down to SO(2) \times SO(3).

PSG classification is the same as the spin- $\frac{1}{2}$ Schwinger boson approach, and we can just quote the results of Wang *et al.* in Ref. [42]. The PSG is labeled by (p_1, p_2, p_3) where $p_1, p_2, p_3 = 0, 1$. These three integers label the fractionalization of the translation σ and C_6 : $T_1 T_2 = T_2 T_1 (-1)^{p_1}$, $\sigma^2 = (-1)^{p_2}$, and $C_6^6 = (-1)^{p_3}$.

For each symmetry operation X , the corresponding projective symmetry operation is $G_X X$ where $G_X = e^{i\varphi_X(\mathbf{r})}$ is a U(1) gauge transformation:

$$\begin{aligned} \varphi_{T_1}(x, y) &= 0, \\ \varphi_{T_2}(x, y) &= p_1 \pi x, \\ \varphi_\sigma(x, y) &= p_2 \frac{\pi}{2} + p_1 \pi xy, \\ \varphi_{C_6}(x, y) &= p_3 \frac{\pi}{2} + p_1 \pi \left(xy + \frac{y(y-1)}{2} \right), \end{aligned} \quad (14)$$

where the coordinate of a site is $\mathbf{R} = x\mathbf{a}_1 + y\mathbf{a}_2$. The transformation of crystal symmetries can be found in Appendix A.

For both Schwinger boson and Schwinger fermion, there are eight different Z_2 spin liquids labeled by (p_1, p_2, p_3) . However, more constraints need to be added if we require the nearest-neighbor pairing to be nonzero. This is a reasonable requirement for a model with dominant nearest-neighbor antiferromagnetic coupling. It turns out there are only two Z_2 spin liquids for both fermion and boson parton in the SO(6)-symmetric limit. In the following, we will introduce

the two PSG *Ansätze* for the Schwinger boson and Schwinger fermion, respectively. Then, we will connect the Schwinger fermion and Schwinger boson approaches and show that they describe the same Z_2 spin liquids in terms of f particle and e particle.

1. Z_2 spin liquid in Schwinger fermion parton

The only SO(6)-symmetric pairing is $\Delta(\mathbf{R}) \sum_a \Psi_a(\mathbf{r})\Psi_a(\mathbf{r} + \mathbf{R})$ where $a = 1, \dots, 6$ is the flavor index. For fermion we have $\Delta(\mathbf{R}) = -\Delta(-\mathbf{R})$. We require $\Delta(\mathbf{R}) \neq 0$ for nearest neighbor \mathbf{R} . First, the reflection σ maps $\mathbf{R} = (1, 1)$ to itself. Under the PSG, $\Delta(1, 1) \rightarrow \Delta(1, 1)e^{i[\varphi_\sigma(0,0) + \varphi_\sigma(1,1)]}$. To have $\Delta(1, 1) \neq 0$, we need $\varphi_\sigma(0, 0) + \varphi_\sigma(1, 1) = 0 \pmod{2\pi}$. This is equivalent to $p_1 = p_2$.

Second, $\mathbf{R}_2 = (-1, 0)$ is related to $\mathbf{R}_1 = (1, 0)$ by three C_6 rotations. Meanwhile, we have $\Delta(-1, 0) = -\Delta(1, 0)$. Therefore, we have the following condition:

$$3\varphi_{C_6}(0, 0) + \varphi_{C_6}(1, 1) + \varphi_{C_6}(0, 1) + \varphi_{C_6}(-1, 0) = \pi \pmod{2\pi}, \quad (15)$$

which requires $p_3 = 1 - p_1 \pmod{2}$. Because of the above two constraints, there are only two reasonable symmetric Z_2 spin liquids with SO(6) rotation symmetry. They are (0,0,1) and (1,1,0) phases. The first is a zero-flux phase while the second is a π -flux phase.

Next, we show that $p_1 = 1$ forbids nearest-neighbor hopping. Consider the hopping $t(\mathbf{R}) \sum_a \Psi_a^\dagger(\mathbf{r} + \mathbf{R})\Psi_a(\mathbf{r})$. $\mathbf{R}_1 = (0, 1)$ and $\mathbf{R}_2 = (1, 0)$ are related by σ or C_6^2 . To have nonzero nearest-neighbor hopping, we need to have

$$\begin{aligned} & -\varphi_\sigma(0, 1) + \varphi_\sigma(0, 0) \\ & = -\varphi_{C_6}(1, 1) - \varphi_{C_6}(0, 1) + 2\varphi_{C_6}(0, 0) \pmod{2\pi} \end{aligned} \quad (16)$$

which fixes $p_1 = 0$. As a result, the π -flux phase needs to have zero nearest-neighbor hopping.

2. Z_2 spin liquid in Schwinger boson parton

For six-flavor bosons, the pairing is also $\Delta(\mathbf{R}) \sum_a \Psi_a(\mathbf{r})\Psi_a(\mathbf{r} + \mathbf{R})$ for each bond \mathbf{R} . We have $\Delta(\mathbf{R}) = \Delta(-\mathbf{R})$. Similar to the fermion case, the reflection σ fixes $p_1 = p_2$. The C_6^3 relates $\mathbf{R}_1 = (1, 0)$ to $\mathbf{R}_2 = (-1, 0)$ and fixes $p_3 = p_1$. There are also two symmetric spin liquids satisfying the following constraint: the zero-flux phase (0,0,0) and the π -flux phase (1,1,1). Again, the π -flux phase can not have nonzero nearest-neighbor hopping.

3. Equivalence between Schwinger boson and Schwinger fermion descriptions

We have found two symmetric Z_2 spin liquids from both Schwinger boson and Schwinger fermion construction. In this section we show that the Schwinger fermion descriptions are equivalent to the Schwinger boson approach.

In the Schwinger boson approach, we have the PSG for the bosonic e particle. In the Schwinger fermion parton theory, we have the PSG for the fermionic $f = ev$. Here, v denotes the vison or m particle. The PSG of f particle can be derived from the composition of the PSG of the e and m particles (with possible twisting factor) [43–45]. There is one e particle per

TABLE II. Two symmetric Z_2 spin liquids. P^b and P^f label symmetric fractionalization for e and f particles. We also list the band bottom of e particle in the Schwinger boson mean field *Ansatz* with only nearest-neighbor coupling.

Phase	PSG	Band bottom of e
Type I Z_2	$P^b = (0, 0, 0), P^f = (1, 1, 0)$	(0,0)
Type II Z_2	$P^b = (1, 1, 1), P^f = (0, 0, 1)$	$\pm(\frac{\pi}{6}, \frac{\pi}{2\sqrt{3}}), \pm(\frac{5\pi}{6}, \frac{\pi}{2\sqrt{3}})$

unit cell and the vison v always see the e particle as an effective π flux. Thus, the vison always has the PSG $T_1 T_2 = -T_2 T_1$ and $C_6^6 = -1$. It has been shown that $\sigma^2 = -1$ is anomalous for the vison when there is a U(1) spin rotation symmetry. Vison must have $\sigma^2 = 1$ [46] in our problem. For the fractionalization of $X = T_1 T_2 (T_2 T_1)^{-1}$, σ^2 , C_6^6 , the PSG of vison $(-1)^{P_X^v}$ can be uniquely determined as $P^v = (-1, 0, -1)$. We can then get PSG of f from the PSG of e particle by $(-1)^{P_X^f} = (-1)^{P_X^e} (-1)^{P_X^v} (-1)^{\epsilon(X)}$, where $\epsilon(X) = 1, -1$ is a twist factor. It has been shown that $\epsilon(T_1 T_2 (T_2 T_1)^{-1}) = 1$ and $\epsilon(\sigma^2) = \epsilon(C_6^6) = -1$ [44,45]. We can then map PSG of e particle $P^b = (p_1^b, p_2^b, p_3^b)$ to $P^f = (p_1^f, p_2^f, p_3^f)$ by the equation

$$p_1^f = p_1^b + 1, \quad p_2^f = p_2^b + 1, \quad p_3^f = p_3^b. \quad (17)$$

From the above relation we can see that both Schwinger boson theory and Schwinger fermion theory are describing two symmetric Z_2 spin liquids: I. $P^b = (0, 0, 0)$ and $P^f = (1, 1, 0)$. II. $P^b = (1, 1, 1)$ and $P^f = (0, 0, 1)$.

In summary, we find two symmetric Z_2 spin liquid, shown in Table II. Each of them can be described using either Schwinger boson or Schwinger fermion mean field *Ansatz*. Details about the *Ansatz* and the dispersion can be found in Appendix C.

V. PSEUDOGAP METALS AT $\nu_T = 2 - x$

After discussing the Mott insulator, we turn to possible metallic phases upon doping the Mott insulator. Especially, we show that pseudogap metals with small Fermi surfaces can naturally emerge upon doping the Mott insulator at $\nu_T = 2$. The Mott insulating phase at $\nu_T = 2$ is sensitive to the onsite intervalley spin-spin coupling J_H . A nonzero J_H split the SO(6) symmetry down to $1 \oplus 2 \oplus 3$. When $J_H > 0$ and its magnitude is much larger than J , it is obvious that the ground state is a featureless Mott insulator with one valley triplet, spin singlet at each site. When $J_H < 0$, with a large magnitude, the low energy is dominated by one SO(3) vector at each site. Therefore, we have an effective spin-one model on triangular lattice and the ground state is the 120° Neel order. For the intermediate region with $J_H = 0$, valence bond solid (VBS) or resonant valence bond (RVB) may also be possible.

In the remaining part we discuss possible metallic phases upon doping from the featureless Mott insulator and the VBS/RVB phase. The physics of doping the Neel order is very hard and we leave it to future work.

A. $J_H > 0$: Symmetric and featureless pseudogap metal

In the simplest case, let us assume $J_H > 0$ and is much larger than J . In this case, the Mott insulator has one

intervalley singlet at each site. When we dope the system to the filling $\nu_T = 2 - x$, there are x singlons. One natural state is that these singlons move coherently and form four Fermi surfaces, each of which has area $A_{\text{FS}} = -\frac{x}{4}$. The remaining particles are still gapped out by singlet formation. Obviously, this is a pseudogap metal with only a small Fermi surface. The Hall number is opposite to the free-fermion case and is proportional to x . This is quite similar to the phenomenology of cuprates when superconductivity is suppressed by strong magnetic field. This pseudogap metal is a symmetric Fermi liquid. Although the picture is very simple, this state is definitely beyond the conventional scenario with density wave order. The existence of this simple example is a proof that electrons can be gapped out from the Fermi sea without invoking any symmetry-breaking order.

Although we can not describe this featureless pseudogap phase with the conventional mean field theory, we find that the essential physics can be easily captured by a slave-boson mean field theory. When we remove one electron from $\nu_T = 2$, we remove one doublon and create one singlon, therefore, we use the following parton representation:

$$c_\alpha(\mathbf{x}) = \sum_{\beta \neq \alpha} \Phi_{\alpha\beta}(\mathbf{x}) f_\beta^\dagger(\mathbf{x}), \quad (18)$$

where $\alpha, \beta = 1, 2, 3, 4$ is the flavor index. $\Phi_{\alpha\beta}(\mathbf{x}) = -\Phi_{\beta\alpha}(\mathbf{x})$ is an antisymmetric slave-boson field, which has been used before in Eq. (9). $f_\beta^\dagger(\mathbf{x})$ creates a singlon with flavor β . The above parton construction has a U(1) redundancy:

$$\Phi_{\alpha\beta}(\mathbf{x}) \rightarrow \Phi_{\alpha\beta}(\mathbf{x}) e^{i\theta(\mathbf{x})}, \quad f_\beta(\mathbf{x}) \rightarrow f_\beta(\mathbf{x}) e^{i\theta(\mathbf{x})} \quad (19)$$

with the constraint $n_f(\mathbf{x}) + n_b(\mathbf{x}) = 1$.

When $J_H = 0$, these six $\Phi_{\alpha\beta}$ fields can form a SO(6) vector in the basis defined in Eq. (9). In the following, we use the SO(6) basis $b_a(\mathbf{x})$ with $a = 1, 2, \dots, 6$:

$$\begin{aligned} b_1 &= \frac{i}{\sqrt{2}}(-\Phi_{12} + \Phi_{34}), \\ b_2 &= \frac{1}{\sqrt{2}}(\Phi_{12} + \Phi_{34}), \\ b_3 &= \frac{i}{\sqrt{2}}(-\Phi_{14} + \Phi_{23}), \\ b_4 &= \frac{1}{\sqrt{2}}(\Phi_{14} + \Phi_{23}), \\ b_5 &= \frac{1}{\sqrt{2}}(\Phi_{13} - \Phi_{24}), \\ b_6 &= -\frac{i}{\sqrt{2}}(\Phi_{13} + \Phi_{24}). \end{aligned} \quad (20)$$

We can substitute Eq. (20) to the t - J model in Eq. (8) and decouple it in the form of mean field theory:

$$\begin{aligned} H_M &= H_b + H_f, \\ H_b &= -t_b \sum_{(ij)} \sum_a b_{a;i}^\dagger b_{a;j} + \text{H.c.} - \mu \sum_i \sum_a b_{a;i}^\dagger b_{a;i}, \\ H_f &= -t_f \sum_{(ij)} \sum_\alpha f_{\alpha;i}^\dagger f_{\alpha;j} + \text{H.c.} - \mu_f \sum_i \sum_\alpha f_{\alpha;i}^\dagger f_{\alpha;i}. \end{aligned} \quad (21)$$

When we add a $J_H > 0$, the degeneracy of the six-flavor bosons is lifted and the one corresponding to the intervalley singlet is favored. This is $b_3 = \frac{i}{\sqrt{2}}(-\Phi_{14} + \Phi_{23})$ defined in Eq. (20). Therefore, we consider the *Ansatz* with $\langle b_3(\mathbf{x}) \rangle \neq 0$. After the condensation of b , the internal U(1) gauge field is Higgsed and f can be identified as a local hole operator c^\dagger . The density of fermion f is $n_f = x$. We have four Fermi surfaces with Fermi surface area $A_{\text{FS}} = -\frac{x}{4}$.

To further prove the phase is a Fermi liquid, we can try to calculate the single Green function. With simple algebras, we can easily get

$$\begin{aligned} G_{\alpha_1, \alpha_2}^c(x, t; y, t') &= \langle c_{\alpha_1}^\dagger(x, t) c_{\alpha_2}(y, t') \rangle \\ &= \sum_{\beta_1 \neq \alpha_1} \sum_{\beta_2 \neq \alpha_2} \langle \Phi_{\alpha_1 \beta_1}^\dagger(x, t) \Phi_{\alpha_2 \beta_2}(y, t') \rangle \langle f_{\beta_1}(x, t) f_{\beta_2}^\dagger(y, t') \rangle \\ &= \sum_{\beta \neq \alpha_1, \alpha_2} \langle \Phi_{\alpha_1 \beta}^\dagger(x, t) \Phi_{\alpha_2 \beta}(y, t') \rangle G_\beta^f(x, t; y, t'). \end{aligned} \quad (22)$$

Using the fact that $\langle \Phi_{14} \rangle = -\langle \Phi_{23} \rangle = \frac{i}{\sqrt{2}} \langle b_4 \rangle$ while other components of $\Phi_{\alpha\beta}$ are zero, we can easily get

$$\begin{aligned} G_{11}^c(x, t; y, t') &= \frac{1}{2} |\langle b \rangle|^2 G_{44}^f(x, t; y, t'), \\ G_{22}^c(x, t; y, t') &= \frac{1}{2} |\langle b \rangle|^2 G_{33}^f(x, t; y, t'), \\ G_{33}^c(x, t; y, t') &= \frac{1}{2} |\langle b \rangle|^2 G_{22}^f(x, t; y, t'), \\ G_{44}^c(x, t; y, t') &= \frac{1}{2} |\langle b \rangle|^2 G_{11}^f(x, t; y, t'). \end{aligned} \quad (23)$$

These equations also mean that the f operator should be identified as a physical hole operator.

In summary, in the limit with a large anti-intervalley Hund's coupling, a natural state in the underdoped regime is a symmetric and featureless Fermi liquid with small Fermi surfaces. Such a state has Hall number $\eta_H = -x$ for $\nu_T = 2 - x$, in contrast to the free-fermion case with $\eta_H = 2 - x$. This simple state offers a simple example to partially gap out free-fermion Fermi surfaces by symmetric singlet formation, instead of the more familiar density wave order.

B. $J_H = 0$: Orthogonal metal with small Fermi surfaces

Next, we turn to the case with $J_H = 0$. In this U(4)-symmetric point, Luttinger theorem requires $A_{\text{FS}} = \frac{\nu_T}{4}$ for a symmetric and featureless phase. However, we will argue that an exotic symmetric pseudogap metal may be possible when doping away from the $\nu_T = 2$ Mott insulator in the $U \gg t$ limit. We will generalize the conventional RVB theory [37] to the type II t - J model close to $\nu_T = 2$. As in the familiar RVB theory, we assume the undoped state is a Z_2 spin liquid.

We still use the parton construction in Eq. (18). We have $n_f = x$ and $n_b = 1 - x$. In the undoped Mott insulator, there are two Z_2 spin liquids as we proposed before. For simplicity, we just use the zero-flux *Ansatz* from the Schwinger boson method. Basically, the Schwinger boson b is in a paired superfluid phase. Then, we dope the system, f can form four Fermi surfaces with area $A_{\text{FS}} = -\frac{x}{4}$ as in the featureless pseudogap metal in the previous subsection. In this mean field *Ansatz*, $\langle b_i b_j \rangle \neq 0$ Higgs the internal U(1) gauge field down to Z_2 . As argued in Ref. [34], in this case the physical charge is carried by fermion f . In another way, we can use Ioffe-Larkin rule for

physical resistivity [47]: $\rho_c = \rho_b + \rho_f$. Because the boson b is in a paired superfluid phase, $\rho_b = 0$, therefore, $\rho_c = \rho_f$. We conclude that the transport property of this phase is exactly the same as a Fermi liquid with small Fermi surfaces. Obviously, we will also expect Hall number $\eta_H = -x$ as in the featureless pseudogap metal. The thermodynamic property, like specific heat or spin susceptibility, should still be the same as the featureless pseudogap metal. Therefore, we still view this phase as a “pseudogap metal” because the number of carriers is much smaller than the conventional Fermi liquid.

Next, we will show that this pseudogap metal is a non-Fermi-liquid (NFL) instead of a Fermi liquid in terms of single-electron Green function. Following the same analysis as in the previous subsection, we can get $G^c(x, y; t, t') \propto \langle b^\dagger(x, t)b(y, t') \rangle G^f(x, y; t, t')$, where we have suppressed the flavor index for simplicity. Because the Schwinger boson b is in a paired-superfluid phase, a single-particle Green function $\langle b^\dagger(x, t)b(y, t') \rangle$ should be an exponential decay. As a result, a single Green function for the physical electron $G^c(x, y; t, t')$ should also be an exponential decay. As a consequence, ARPES or STM measurement can not detect any coherent quasiparticle for this pseudogap metal. The charge carrier in this exotic metal is not the physical electron. We will follow the notation of Ref. [34] and dub it as “orthogonal metal.”

In summary, we have shown that a featureless pseudogap metal or an orthogonal metal with small Fermi surfaces $A_{FS} = -\frac{x}{4}$ can naturally emerge at filling $\nu_T = 2 - x$ for large positive J_H or small J_H . For a negative and large J_H , we know that the $\nu_T = 2$ Mott insulator is in the 120° Neel order for the low-energy spin-one model. Doping such a Neel order may show a new metallic or superconducting phase beyond the analysis here, which we leave to future work.

VI. DECONFINED METAL BETWEEN PSEUDOGAP METAL AND CONVENTIONAL FERMI LIQUID

At the large $U \gg t$ limit, we have argued that a pseudogap metal with small Fermi surfaces is likely at small doping away from $\nu_T = 2$. Then, a natural question is how this small Fermi surface pseudogap metal evolves to the conventional Fermi liquid with large Fermi surfaces when increasing $\frac{t}{U}$ or the doping x . We try to provide one possible scenario in this section.

For simplicity, we work in the case with $J_H = 0$. We have already presented a description of the orthogonal metal with small Fermi surfaces. Next, we need to understand how to describe the conventional Fermi liquid with large Fermi surfaces. At large $\frac{t}{U}$, this is a trivial problem. At the large $U \gg t$ with large doping x , we still expect a conventional Fermi liquid, which can not be simply understood as in the free-fermion case because of the constraint P_2 in Eq. (8). In the familiar spin- $\frac{1}{2}$ case or in the filling $\nu_T = 1 - x$ of the U(4) model, the constraint in Eq. (7) can be respected in the slave-boson description: $c_\alpha(\mathbf{x}) = b^\dagger(\mathbf{x})f_\alpha(\mathbf{x})$. Then, the conventional Fermi liquid just corresponds to the *Ansatz* with $\langle b(\mathbf{x}) \rangle \neq 0$. In contrast, in the case $\nu_T = 2 - x$, the Hilbert space consists of singlon and doublon. Neither of them can simply condense without breaking spin rotation symmetry. Meanwhile, the density of a singlon is x while the number of a doublon is $1 - x$. Therefore, to have the conventional

Fermi liquid with Hall number $\eta_H = 2 - x$, we need both singlons and doublons to be absorbed to form the large Fermi surface with area $A_{FS} = \frac{2-x}{4}$. In the following, we will show that a large Fermi surface state can be generated from “Kondo resonance” similar to heavy-fermion systems.

To impose the constraint P_2 in Eq. (8), we still use the parton construction in Eq. (18). With this parton construction, we can define spin operators for the doublon site using the slave boson b_a (linear transformation of $\Phi_{\alpha\beta}$) and the spin operators for the singlon site using the fermion f .

The spin operator for the doublon site is

$$S_b^{ab}(\mathbf{x}) = 2i[b_a^\dagger(\mathbf{x})b_b(\mathbf{x}) - b_b^\dagger(\mathbf{x})b_a(\mathbf{x})], \quad (24)$$

where $a, b = 1, 2, \dots, 6$. S^{ab} is the generator of the SO(6) group. It has a one-to-one correspondence to the SU(4) spin operators as defined in Table I.

The spin operator for the singlon site is

$$S_f^{\mu\nu}(\mathbf{x}) = f_\alpha^\dagger \tau^\mu \sigma^\nu f_\beta(\mathbf{x}), \quad (25)$$

where $\alpha, \beta = 1, 2, 3, 4$. $\tau^\mu \sigma^\nu$ with $\mu, \nu = 0, x, y, z$ except $\mu = \nu = 0$.

With this six-flavor slave-boson parton construction, the t term in the t - J model defined in Eq. (8) looks like an exchange term between the singlon f and the doublon b : $b_i^\dagger b_j f_i f_j^\dagger$. Here, we suppressed the flavor index because generically it looks quite complicated and involves many different terms. This term can be decoupled to the mean field *Ansatz* in Eq. (21). The J term in this case involves terms like $S_{b;i} S_{b;j}$, $S_{f;i} S_{f;j}$, and $S_{b;i} S_{f;j}$. At small doping x , we have $n_b = 1 - x$ and $n_f = x$. In this case, we can view the doublon site as a SO(6) spin and the fermion f couples to the SO(6) moment through the term $S_{b;i} S_{f;j}$, which resembles a Kondo coupling in the heavy-fermion problem. Then, a large Fermi surface may be generated through “Kondo resonance.”

The essential point of Kondo resonance is to absorb the SO(6) spin to form a large Fermi surface with area $A_{FS} = \frac{2-x}{4}$. To do that, we need to split a doublon to two fermions first. Therefore, we do a further parton construction on top of Eq. (18):

$$\Phi_{\alpha\beta} = \frac{1}{2}[\psi_\alpha(\mathbf{x})\psi_\beta(\mathbf{x}) - \psi_\beta(\mathbf{x})\psi_\alpha(\mathbf{x})]. \quad (26)$$

In other words, the original electron operator is now written

$$c_\alpha(\mathbf{x}) = \sum_{\beta \neq \alpha} \psi_\alpha(\mathbf{x})\psi_\beta(\mathbf{x})f_\beta^\dagger(\mathbf{x}) \quad (27)$$

with the constraint $\frac{1}{2}n_\psi(\mathbf{x}) + n_f(\mathbf{x}) = 1$. Still, there is a U(1) gauge redundancy

$$f_\alpha(\mathbf{x}) \rightarrow f_\alpha(\mathbf{x})e^{i\varphi(\mathbf{x})}, \quad \psi_\alpha(\mathbf{x}) \rightarrow e^{i\frac{1}{2}\varphi(\mathbf{x})}. \quad (28)$$

So, ψ couples to the U(1) gauge field \mathbf{a} with gauge charge $\frac{1}{2}$. In addition, ψ couples to another Z_2 gauge field because $\psi_\alpha(\mathbf{x}) \rightarrow -\psi_\alpha(\mathbf{x})$ also does not change the physical operator.

With the parton construction in Eq. (27), we can access both the conventional Fermi liquid and the pseudogap metals with small Fermi surfaces. For simplicity, let us assume that the physical gauge field \mathbf{A} couples to f . It turns out that the conventional Fermi liquid can evolve to the pseudogap metal through two continuous transitions with an intermediate “deconfined metal,” as is illustrated in Fig. 4. We have density

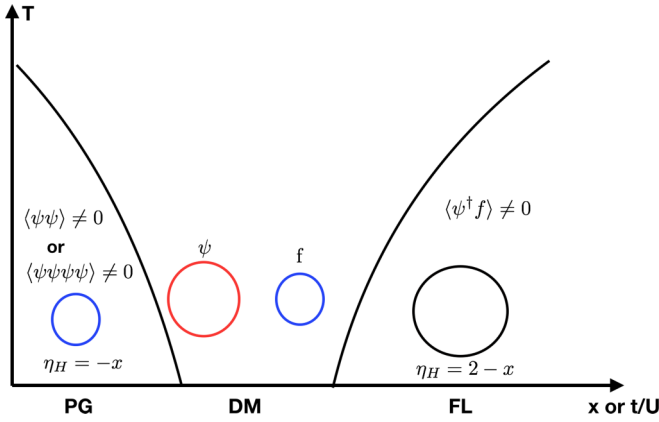


FIG. 4. Evolution from pseudogap metal to the conventional Fermi liquid. The red, blue, and black circles denote Fermi surfaces with area $\frac{2-2x}{4}$, $\frac{x}{4}$, and $\frac{2-x}{4}$. The intermediate phase is a “deconfined metal” where the Fermi surfaces formed by ψ and f couple to an internal U(1) gauge field \mathbf{a} . We can condense either $\psi\psi V$ or $\psi\psi\psi\psi V$ to get featureless pseudogap metal or orthogonal pseudogap metal, where V is the vison annihilation operator.

$n_\psi = 2 - 2x$ and $n_f = x$. The conventional Fermi liquid is described by $\langle\psi^\dagger f\rangle \neq 0$, similar to the Kondo resonance in the heavy-fermion problems. To get the pseudogap metal, we can just gap out the Fermi surfaces formed by ψ through pairing. The first possibility is a charge- $2e$ pairing $\langle\psi\psi\rangle \neq 0$. In the case with $J_H = 0$, this pairing term needs to break the SU(4) spin rotation and lives in a manifold generated by SO(6) rotation. If $J_H > 0$, we can just make ψ to form the intervalley, spin-singlet pairing which preserves spin rotation symmetry. The pairing term will completely Higgs the U(1) gauge field \mathbf{a} . However, the Z_2 gauge field still survives and decouples with the remaining Fermi surfaces formed by f . This is actually a FL* phase with Fermi liquid coexisted with Z_2 gauge field. To avoid such an exotic state and get the featureless pseudogap metal, we should condense $\langle\psi\psi\psi V\rangle \neq 0$ where V is the vison of the Z_2 gauge field. In this way, the Z_2 gauge field also gets confined and we get exactly the featureless pseudogap metal. In the SU(4)-symmetric point, the orthogonal pseudogap metal may be favored. We can reach it through a charge- $4e$ SU(4) singlet pairing: $\langle\epsilon_{\alpha\beta\gamma\delta}\psi_\alpha\psi_\beta\psi_\gamma\psi_\delta V\rangle \neq 0$. This pairing Higgses the U(1) gauge field \mathbf{a} down to Z_2 . Therefore, the Fermi surface from f couples to both A and the Z_2 gauge field, which is exactly the property of the orthogonal pseudogap metal described in the previous section.

Now, we have one theory that the pseudogap metal can evolve to the Fermi liquid through two continuous phase transitions. Next, we briefly discuss the property of the intermediate deconfined metal. The low-energy physics is governed by the following action:

$$\begin{aligned}
 L = & \psi^\dagger \left(\partial_0 - \frac{1}{2} a_0 \right) \psi + f^\dagger (\partial_0 - a_0) f \\
 & + \frac{\hbar^2}{2m_\psi} \psi^\dagger \left(-i\vec{\partial} - \frac{1}{2}\vec{a} \right)^2 \psi \\
 & + \frac{\hbar^2}{2m_f} f^\dagger (-i\vec{\partial} + \vec{A} - \vec{a})^2 f.
 \end{aligned} \quad (29)$$

In the Gaussian approximation, an Ioffe-Larkin rule can be easily derived as

$$\rho_c = \rho_\psi + \rho_f, \quad (30)$$

where ρ_ψ and ρ_f should be viewed as the resistivity tensor for ψ and f .

Because of the gauge fluctuation, the quasiparticle picture is known to break down. Transport of such a deconfined metal remains to be an unsolved theoretical problem. We hope that the possible realization of this phase in graphene moiré superlattice can provide more information from experiment on this problem.

When applying an external magnetic field, we can get an effective action for the internal magnetic flux:

$$L_{\text{eff}} = \chi_\psi \left| \frac{1}{2} b \right|^2 + \chi_f |b - B|^2. \quad (31)$$

In the saddle point, the internal gauge field flux \mathbf{b} is locked to the external magnetic field: $\mathbf{b} = \alpha \mathbf{B}$ with $\alpha = \frac{4\chi_f}{\chi_\psi + 4\chi_f}$. Here, χ_ψ and χ_f are the diamagnetism susceptibility in the Gaussian approximation. Generically, we expect α is an order one number smaller than one. Using $\chi \sim \frac{1}{m}$ for a Fermi surface, we have $\alpha = \frac{4m_\psi}{4m_\psi + m_f}$. Because of the locking, ψ sees an effective field $\alpha \mathbf{B}$ while f sees an effective field $-(1 - \alpha) \mathbf{B}$. Then, in principle, one should see quantum oscillations corresponding to the Fermi surfaces area for both ψ and f with frequency renormalized by factor α and $1 - \alpha$.

Next, we discuss the Hall number of this deconfined metal. The constraint $\frac{1}{2}n_\psi + n_f = 1$ implies that $\mathbf{J}_\psi = \mathbf{J}_f$, where $\mathbf{J}_\psi = \mathbf{J}$ is defined as variation of \mathbf{a} while \mathbf{J}_f is defined as variation of \mathbf{A} . In the Gaussian approximation, we have the result

$$\begin{aligned}
 e_x &= \frac{\alpha B}{n_\psi \frac{1}{2} e} J_y^\psi, \\
 e_x - E_x &= \frac{1 - \alpha}{n_f e} B J_y^f,
 \end{aligned} \quad (32)$$

where we have used the result $\rho_{xy} = \frac{B}{nQ}$ for a Fermi surface with charge Q and density n .

Then, it is easy to get

$$E_x = \left(\frac{2\alpha}{n_\psi e} - \frac{1 - \alpha}{n_f e} \right) B J_y. \quad (33)$$

Therefore, the Hall number is

$$\frac{1}{\eta_H} = \left(\frac{2\alpha}{n_\psi} - \frac{1 - \alpha}{n_f} \right) \quad (34)$$

or

$$\eta_H = \left(\frac{\alpha}{1 - x} - \frac{1 - \alpha}{x} \right)^{-1}. \quad (35)$$

Note that, generically, η_H is not related to the density of charge carriers. At the limit $x \ll 1$ and $\alpha \ll 1$, we have $\eta_H \approx -\frac{x}{1 - \alpha}$. η_H diverges when α increases to $1 - x$. Therefore, the Hall number can be arbitrary inside the deconfined metal, depending on the value of α .

Once the system is in the FL phase, $\langle\psi^\dagger f\rangle$ locks $\mathbf{a} = 2\mathbf{A}$. In this case, ψ forms an electron pocket while f can be viewed

as a hole pocket. Deep inside the FL phase, the two Fermi surfaces merge together to form a large electron Fermi surface and $\eta_H = 2 - x$.

In the above we have described one scenario for evolution from pseudogap metals to conventional Fermi liquid by increasing doping or bandwidth. In this simple scenario, there is an intermediate deconfined metal phase. The physics of the pseudogap metal we described is kind of similar to the ‘‘symmetric mass generation’’ proposed in Ref. [48] for Dirac fermions. In that simple, case Ref. [48] constructed a deconfined critical point between an insulator and a Dirac semimetal. It is not clear whether a direct transition between the pseudogap metal and the conventional Fermi liquid can exist or not in our case. We hope to study this in the future.

VII. U(1) SPINON FERMION SURFACE STATE AND Z_4 SPIN LIQUID AT $\nu_T = 1$

At $\nu_T = 1$, the intervalley Hund’s term J_H vanishes after projection to the Hilbert space without double occupancy. Therefore, the spin rotation symmetry is $SU(4)/Z_4$ or $U(1)_{\text{valley}} \times SO(3)_+ \times SO(3)_-$. We will show that there is no symmetric gapped Z_2 spin liquid when spin rotation symmetry is both $SU(4)/Z_4$ and $U(1)_{\text{valley}} \times SO(3)_+ \times SO(3)_-$. Within the Abrikosov fermion parton construction, the only symmetric spin-liquid state is a U(1) spin liquid with spinon Fermi surface, which can be reached from the Fermi-liquid phase through a continuous transition. A symmetric Z_4 spin liquid is also possible but beyond mean field description.

A. Absence of gapped symmetric Z_2 spin liquid

There is a general argument to rule out gapped Z_2 spin liquid with full spin rotation symmetry. Because there is only one fundamental representation within each unit cell, in a spin rotation invariant Z_2 spin liquid, the spinon needs to transform as $(\frac{1}{2}, 0)$ and $(0, \frac{1}{2})$ under $SU(2)_+ \times SU(2)_-$. Basically, we have $e_{+\sigma}$ carries valley + and $e_{-\sigma}$ carries valley -. A bound state formed by $e_{+\sigma_1}e_{-\sigma_2}$ has dimension 4 and transforms as $(\frac{1}{2}, \frac{1}{2})$ under $SU(2)_+ \times SU(2)_-$. Under 2π rotation of S_z for either valley, it acquires a global -1 phase. Therefore, the bound state is in the projective representation of $U(1)_{\text{valley}} \times SO(3)_+ \times SO(3)_-$. However, in a gapped Z_2 spin liquid, e_+e_- is created by a local operator and should be in a linear representation. The contradiction implies that a gapped symmetric Z_2 spin liquid is not possible.

B. U(1) spin liquid in Abrikosov fermion parton construction

A U(1) spin liquid is possible and can be constructed in the standard Abrikosov fermion parton theory. For the current problem, Schwinger boson parton theory is not very useful because there is no symmetric paired condensation phase of the four-flavor Schwinger bosons. Therefore, we restrict to Abrikosov fermion parton theory. At each site, we have f_{ia} in the fundamental representation of $SU(4)$ with the constraint $\sum_a f_{ia}^\dagger f_{ia} = 1$. Unlike the spin- $\frac{1}{2}$ case, there is only a U(1) gauge redundancy.

Apparently, there can not be pairing term which preserves the spin rotation symmetry. This is another manifestation that

symmetric Z_2 spin liquid is not possible. In the following, we classify all possible symmetric U(1) spin-liquid states.

The projective symmetric group (PSG) for U(1) spin liquid is classified in Appendix B. There are only two possible PSG, which are labeled by the projective translation symmetry: $T_1 T_2 = T_2 T_1 e^{i\Phi_T}$. It turns out only $\Phi_T = 0$ and $\Phi_T = \pi$ are compatible with the reflection symmetry σ . Once Φ_T is fixed, the symmetry realizations of σ and C_6 are also fixed. Note that C_6^6 and σ^2 are meaningless in a U(1) spin liquid because a global U(1) transformation can always be added in C_6 and σ . For each symmetry operation X , the symmetry realization is $e^{i\varphi_X(x,y)} X$. The following is a list of the PSG:

$$\begin{aligned}\varphi_{T_1} &= 0, \\ \varphi_{T_2} &= p_1 \pi x, \\ \varphi_\sigma &= p_1 \pi xy, \\ \varphi_{C_6} &= p_1 \pi xy + \frac{1}{2} p_1 \pi y(y-1)\end{aligned}\quad (36)$$

up to a constant phase. $\Phi_T = p_1 \pi$ with $p_1 = 0, 1$. $p_1 = 0$ and $p_1 = 1$ label the zero-flux phase and the π -flux phase. However, in the π -flux phase the nearest-neighbor hopping and the next-nearest-neighbor hopping are forbidden. This *Ansatz* is not energetically favorable. Therefore, we only consider the zero-flux phase.

In the zero-flux phase, $\varphi_X = 0$. Therefore, all of the symmetry operations are realized trivially. The phase is a U(1) spin liquid with four Fermi surfaces, each at filling $\frac{1}{4}$. This spin-liquid phase can be reached from the Fermi-liquid side through a continuous quantum phase transition. In principle, a symmetric Z_4 spin liquid is also possible. In the Abrikosov fermion description, the fermion can form a charge- $4e$ singlet pairing: $\langle \epsilon_{abcd} f_a f_b f_c f_d \rangle \neq 0$, resulting in a symmetric Z_4 spin liquid.

For the spin-valley model at $\nu_T = 1$, there is no symmetric featureless Mott insulator and magnetic order may be suppressed because of the frustration of triangular lattice and large quantum fluctuation space. The most likely competing ordered state is a plaquette order with four sites forming a $SU(4)$ singlet. If such a plaquette order is melted, we can get a quantum spin-liquid phase. In this case, our PSG analysis suggests a U(1) spin liquid with spinon Fermi surface or a Z_4 spin liquid.

A superconductor has been reported at small doping away from the $\nu_T = 1$ Mott insulator [10]. For both the Z_4 spin liquid and the plaquette order, the Mott insulator is a $SU(4)$ singlet. Therefore, upon doping, the most likely superconductor has charge- $4e$ pairing. A charge- $4e$ superconductor will be killed by in-plane Zeeman field, which is consistent with the experiment [10]. In contrast, a conventional charge- $2e$ pairing lives on a $SO(4)$ manifold because valley triplet, spin singlet pairing is degenerate with the valley singlet, spin triplet pairing. A Zeeman field will select the spin triplet pairing and there is no reason to expect the T_c to be suppressed by Zeeman field. Given the experimental phenomenology and the possible $SU(4)$ -symmetric Mott insulator nearby, the possibility that the observed superconductor is charge- $4e$ paired should be taken seriously. We leave a detailed analysis of charge- $4e$ superconductor to future work.

VIII. CONCLUSION

In this paper, we study possible interesting phases in a spin-valley Hubbard model on triangular moiré superlattice. We show that pseudogap metals with small Fermi surfaces can naturally emerge by doping the $\nu_T = 2$ Mott insulator. In the moiré materials, it is also easy to study the possible transition between the pseudogap metals and the conventional Fermi liquid by tuning either doping or displacement field. We propose one possible route through an intermediate deconfined metallic phase. We also comment on possible spin liquids at $\nu_T = 1$ and charge- $4e$ superconductor nearby. Our proposals can be easily tested in ABC trilayer graphene aligned with hBN and in twisted transition metal dichalcogenide homobilayers. The existence of two distinct symmetric Fermi liquids from symmetry analysis is also true for the graphene moiré systems with topological bands. In the future, it is interesting to study whether a similar symmetric Fermi liquid with small Fermi surfaces can naturally exist in the topological case.

ACKNOWLEDGMENTS

We thank T. Senthil for very helpful discussions. This work was supported by US Department of Energy Grant No. DE-SC000873.

APPENDIX A: CRYSTAL SYMMETRY OF TRIANGULAR LATTICE

We define $\mathbf{r} = x\mathbf{a}_1 + \mathbf{a}_2$. The lattice symmetries are

$$\begin{aligned} T_1 &: (x, y) \rightarrow (x + 1, y), \\ T_2 &: (x, y) \rightarrow (x, y + 1), \\ \sigma &: (x, y) \rightarrow (y, x), \\ C_6 &: (x, y) \rightarrow (x - y, x). \end{aligned} \quad (\text{A1})$$

The following algebraic constraints are useful:

$$\begin{aligned} T_2 T_1 &= T_1 T_2, \\ T_1 C_6 &= C_6 T_2^{-1}, \\ T_2 C_6 &= C_6 T_1 T_2, \\ T_1 \sigma &= \sigma T_2, \\ T_2 \sigma &= \sigma T_1, \\ C_6^6 &= 1, \\ \sigma^2 &= 1, \\ C_6 \sigma &= \sigma C_6^5. \end{aligned} \quad (\text{A2})$$

APPENDIX B: PROJECTIVE SYMMETRY GROUP CLASSIFICATION FOR U(1) SPIN LIQUID

At $\nu_T = 1$, we can use the Abrikosov fermion in the SU(4) fundamental representation. At $\nu_T = 2$, we can have U(1) spin liquid described by a six-flavor Schwinger fermion. In this Appendix we classify all symmetric U(1) spin-liquid states within the fermion parton theory for both $\nu_T = 1$ and 2. First, invariant gauge group (IGG) is $\{e^{i\theta}\}$ where $\theta \in [0, 2\pi)$ is a constant phase. For each

symmetry operation X , we can parametrize the gauge transformation as $G_X(\mathbf{r}) = e^{i\varphi_X(\mathbf{r})}$. Under gauge transformation $G(\mathbf{x}) = e^{i\varphi_G(\mathbf{x})}$, the G_X should be replaced by $GG_XG^{-1}X^{-1}$. Correspondingly we have

$$\varphi_X(\mathbf{r}) \rightarrow \varphi_G(\mathbf{r}) + \varphi_X(\mathbf{r}) - \varphi_G(X^{-1}\mathbf{r}). \quad (\text{B1})$$

Next, we need to fix the gauge. Following Wen and Fa Wang *et al.* [42], we fix $\varphi_{T_1}(\mathbf{r}) = 0$. This can be done by solving the equations

$$\varphi_G(x, y) + \varphi_X(x, y) - \varphi_G(x - 1, y) = 0. \quad (\text{B2})$$

These two equations fix dependence of $G(x, y)$ on x . If $G(0, y)$ is fixed, then $G(x, y)$ is fixed. Now, we only have the gauge freedom $G(0, y)$. Then, we can use $T_1 T_2 = T_2 T_1$ to fix G_{T_2} . Using $T_1^{-1} T_2 T_1 T_2^{-1} = I$, we have

$$\varphi_{T_2}(x, y) = \varphi_{T_2}(0, y) + \Phi_T x, \quad (\text{B3})$$

where $\Phi \in [0, 2\pi)$ is a position-independent constant. We can use the remaining gauge freedom $G(0, y)$ to make $\varphi_{T_2}(0, y) = 0$. Because IGG is U(1), a constant phase in $\varphi_X(x, y)$ does not matter. A nonzero Φ means a projective translation symmetry: $T_2 T_1 = T_1 T_2 e^{i\Phi_T}$. We need to fix $\frac{\Phi_T}{\pi} = \frac{p}{q}$ where p, q are integers.

Next, we need to find PSG for σ and C_6 . First, we need to point out the remaining gauge freedom we can use. The first one is $G_1 : \varphi_1 = \text{const}$. The second one is $G_2 : \varphi_2(x, y) = \theta_2 x$. This will change $\varphi_{T_1} = \theta_2$. However, it belongs to the IGG and does not matter. The third one is $G_3 : \varphi_3(x, y) = \theta_3 y$. This gauge of freedom can be used to eliminate redundant parameters later.

Finally, we get $\varphi_\sigma(x, y) = \Phi_T xy + \text{const}$. From $T_1^{-1} \sigma T_2 \sigma^{-1} = I$ and $T_2^{-1} \sigma T_1 \sigma^{-1} = I$ we have

$$\begin{aligned} \varphi_\sigma(x + 1, y) - \varphi_\sigma(x, y) &= -\Phi_T y + \phi'_2, \\ \varphi_\sigma(x, y + 1) - \varphi_\sigma(x, y) &= \Phi_T x + \phi'_3, \end{aligned} \quad (\text{B4})$$

where ϕ'_2, ϕ'_3 are constant phases.

From these equations we can get $\varphi_\sigma(X, Y) = \varphi_\sigma(0, 0) + \phi'_2 X + \phi'_3 Y + \Phi_T XY \text{ mod } 2\pi = \varphi_\sigma(0, 0) + \phi'_2 X + \phi'_3 Y - \Phi_T XY \text{ mod } 2\pi$. To have solution, we need to fix $\Phi_T = 0, \pi$. Therefore, a general flux Φ is not compatible with the reflection symmetry. In the following, we can use the notation $\Phi_T = p_1 \pi$. A general solution is

$$\varphi_\sigma(x, y) = \varphi_\sigma(0, 0) + p_1 \pi xy + \phi'_2 x + \phi'_3 y. \quad (\text{B5})$$

From $\sigma^2 = I$ we have

$$\varphi_\sigma(x, y) + \varphi_\sigma(y, x) = 2\varphi_\sigma(0, 0), \quad (\text{B6})$$

which fixes $\phi'_2 = -\phi'_3 \text{ mod } 2\pi$.

Now, we can use the gauge freedom $G_2 = e^{i\theta_2 x}$ to reduce the parameters. $\varphi_\sigma(x, y)$ changes to

$$\begin{aligned} \varphi_\sigma(x, y) &\rightarrow \varphi_\sigma(x, y) + \theta_2(x - y) \\ &\rightarrow \varphi_\sigma(0, 0) + p_1 \pi xy + (\phi'_2 + \theta_2)(x - y). \end{aligned} \quad (\text{B7})$$

We can always choose $\theta_2 = -\phi'_2$. Finally, we have the PSG for σ :

$$\varphi_\sigma(x, y) = p_1 \pi xy + \text{const}. \quad (\text{B8})$$

The next task is C_6 . We can still use G_1 and G_2G_3 , which do not change $G_{T_1}, G_{T_2}, G_\sigma$ up to a constant phase. Using $T_1^{-1}C_6T_2^{-1}C_6^{-1} = I$ and $T_2^{-1}C_6T_1T_2C_6^{-1} = I$, we can get

$$\begin{aligned} \varphi_{C_6}(x+1, y) - \varphi_{C_6}(x, y) &= \phi'_4 + p_1\pi y, \\ \varphi_{C_6}(x, y+1) - \varphi_{C_6}(x, y) &= \phi'_5 + p_1\pi(x-y), \end{aligned} \quad (\text{B9})$$

where ϕ'_4, ϕ'_5 are constant U(1) phases. A general solution is

$$\begin{aligned} \varphi_{C_6}(x, y) &= \varphi_{C_6}(0, 0) + p_1\pi xy \\ &\quad - \frac{1}{2}p_1y(y-1)\pi + \phi'_4x + \phi'_5y. \end{aligned} \quad (\text{B10})$$

$C_6\sigma C_6\sigma$ further impose the constraint

$$\varphi_{C_6}(x, y) + \varphi_{C_6}(y-x, y) + \varphi_\sigma(y, y-x) + \varphi_\sigma(y, x) = \text{const}, \quad (\text{B11})$$

which fixes $\phi'_4 + 2\phi'_5 = 0 \pmod{2\pi}$. $C_6^6 = I$ imposes the constraint $\phi'_4 = 0 \pmod{2\pi}$. Then, we can also fix $\phi'_5 = p'_5\pi$ with $p'_5 = 0, 1$.

Under the gauge transformation $G'_3 = e^{i\theta_3(x+y)}$, the solution of φ_{C_6} changes to

$$\begin{aligned} \varphi_{C_6} &\rightarrow \varphi_{C_6}(0, 0) + p_1\pi xy - \frac{1}{2}p_1y(y-1)\pi \\ &\quad + (p'_5\pi - \theta_3)y + 2\theta_3x. \end{aligned} \quad (\text{B12})$$

Choosing $\theta_3 = p'_5\pi$, φ_{C_6} can always be reduced to

$$\varphi_{C_6} = p_1\pi xy + \frac{1}{2}p_1y(y-1)\pi \quad (\text{B13})$$

up to a constant phase.

APPENDIX C: MEAN FIELD OF Z_2 SPIN LIQUID AT $\nu_T = 2$

In this Appendix we analyze the mean field *Ansatz* for SO(6)-symmetric Hamiltonian with only nearest-neighbor coupling J at $\nu_T = 2$ based on the Schwinger fermion and the Schwinger boson parton theories. We focus on the two symmetric Z_2 spin liquids.

1. Type I Z_2 spin liquid

The type I Z_2 spin liquid has PSG $P^b = (0, 0, 0)$ and $P^f = (1, 1, 0)$. The bosonic e spinon has a trivial PSG while the f particle is in a π -flux phase. We can get the dispersions of the e particle and the f particle from the Schwinger boson and the Schwinger fermion mean field theories, respectively.

a. Mean field theory for the bosonic spinon

The dispersion of the e particle is described by the Schwinger boson mean field theory with zero-flux *Ansatz*. We have both nearest-neighbor hopping and pairing terms. Because all of the six bosons decouple with each other in the mean field level, we can work with a spinless boson b at filling $n_b = \frac{1}{6}$ with the Hamiltonian

$$H_b = t \sum_{\langle ij \rangle} b_i^\dagger b_j - \Delta^* \sum_{\langle ij \rangle} (b_i b_j + \text{H.c.}) - \mu \sum_i b_i^\dagger b_i \quad (\text{C1})$$

or in momentum space

$$\begin{aligned} H_b &= \frac{1}{2} \sum_{\mathbf{k}} (b^\dagger(\mathbf{k}), b(-\mathbf{k})) \begin{pmatrix} \xi(\mathbf{k}) & -\Delta(\mathbf{k}) \\ -\Delta^*(\mathbf{k}) & \xi(\mathbf{k}) \end{pmatrix} \begin{pmatrix} b(\mathbf{k}) \\ b^\dagger(-\mathbf{k}) \end{pmatrix} \\ &\quad + \dots, \end{aligned} \quad (\text{C2})$$

where $\Delta(\mathbf{k}) = \sum_{\mathbf{R}} \Delta e^{-i\mathbf{k}\cdot\mathbf{R}}$.

Using the standard Bogoliubov transformation

$$\alpha_{\mathbf{k}} = \mu_{\mathbf{k}} b_{\mathbf{k}} + \nu_{\mathbf{k}} b_{-\mathbf{k}}^\dagger \quad (\text{C3})$$

with the constraint

$$\mu^2(\mathbf{k}) - \nu^2(\mathbf{k}) = 1. \quad (\text{C4})$$

The inverse transformation is

$$b_{\mathbf{k}} = \mu_{\mathbf{k}}^* \alpha_{\mathbf{k}} - \nu_{\mathbf{k}} \alpha_{-\mathbf{k}}^\dagger, \quad (\text{C5})$$

where we assumed $\mu_{\mathbf{k}} = \mu_{-\mathbf{k}}$ and $\nu_{\mathbf{k}} = \nu_{-\mathbf{k}}$.

The solution is

$$\begin{aligned} \mu_{\mathbf{k}}^2 &= \frac{1}{2} \left(\frac{\xi(\mathbf{k})}{E_{\mathbf{k}}} + 1 \right), \\ \nu_{\mathbf{k}}^2 &= \frac{1}{2} \left(\frac{\xi(\mathbf{k})}{E_{\mathbf{k}}} - 1 \right) \end{aligned} \quad (\text{C6})$$

with the sign

$$2\mu_{\mathbf{k}}\nu_{\mathbf{k}} = -\frac{\Delta}{E_{\mathbf{k}}}, \quad (\text{C7})$$

where

$$E_{\mathbf{k}} = \sqrt{\xi_{\mathbf{k}}^2 - \Delta_{\mathbf{k}}^2}. \quad (\text{C8})$$

The final dispersion is

$$H = \frac{1}{2} \sum_{\mathbf{k}} E_{\mathbf{k}} (\alpha_{\mathbf{k}}^\dagger \alpha_{\mathbf{k}} + \alpha_{-\mathbf{k}}^\dagger \alpha_{-\mathbf{k}}) + E_0. \quad (\text{C9})$$

At zero T , the expectation value is $\langle \alpha_{\mathbf{k}}^\dagger \alpha_{\mathbf{k}} \rangle = 0$, which leads to

$$\langle b_{\mathbf{k}}^\dagger b_{\mathbf{k}} \rangle = \nu_{\mathbf{k}}^2 \quad (\text{C10})$$

and

$$\langle b_{\mathbf{k}} b_{-\mathbf{k}} \rangle = -\mu_{\mathbf{k}} \nu_{\mathbf{k}} = \frac{\Delta_{\mathbf{k}}}{2E_{\mathbf{k}}}. \quad (\text{C11})$$

Finally, we get the self-consistent equation

$$\begin{aligned} \frac{1}{N} \sum_{\mathbf{k}} \nu_{\mathbf{k}}^2 &= \frac{1}{6}, \\ t &= 24 \left(1 + \frac{1}{6} \right) J \frac{1}{N} \sum_{\mathbf{k}} \nu_{\mathbf{k}}^2 e^{i\mathbf{k}\cdot\mathbf{a}_1}, \\ \Delta &= 24 \left(1 + \frac{1}{6} \right) J \frac{1}{N} \sum_{\mathbf{k}} \frac{\Delta_{\mathbf{k}}}{2E_{\mathbf{k}}} e^{-i\mathbf{k}\cdot\mathbf{a}_1}, \end{aligned} \quad (\text{C12})$$

where $\mathbf{a}_1 = (1, 0)$ is one bond. The mean field energy is

$$E_M = 28J \sum_{\langle ij \rangle} (\langle b_i^\dagger b_j \rangle^2 - \langle b_i b_j \rangle^2). \quad (\text{C13})$$

For total density $n_b = 0.5/6$, we find an *Ansatz* with $t = 0.795J$ and $\Delta = 3.644J$. Such an *Ansatz* has band bottom at the Γ point. The mean field energy is $E_M = -0.03732 \times 42J$. The critical density for condensation is around 1.45. The condensation of e particle leads to a ferromagnetic state, which is apparently not physical for an antiferromagnetic spin model.

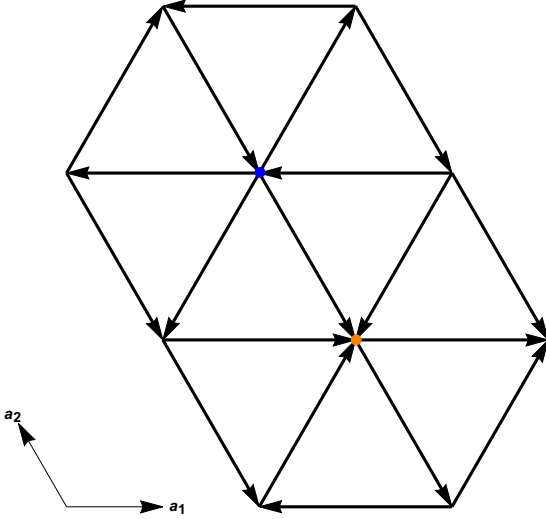


FIG. 5. π -flux Ansatz for Schwinger fermion with nearest-neighbor pairing. The pairing term is odd under inversion. The direction of the arrow denotes the positive pairing.

b. Mean field theory of f particle

The Schwinger fermion mean field theory describes the dispersion of the f particle. The PSG is $P^f = (1, 1, 0)$. It has zero nearest-neighbor hopping while the pairing terms follow a π -flux Ansatz depicted in Fig. 5.

The mean field Ansatz for each component is effectively spinless:

$$H_M = -\mu \sum_i f_i^\dagger f_i - \sum_{\langle ij \rangle} (\Delta_{ij}^* f_i f_j + \text{H.c.}). \quad (\text{C14})$$

We need to fix the filling $\langle f_i^\dagger f_i \rangle = \frac{1}{6}$. The pairing Ansatz is $\Delta_{ij} = -\Delta_{ji}$ with $|\Delta_{ij}| = \Delta$. The π -flux Ansatz has two sublattices A and B . In the momentum space,

$$H = \frac{1}{2} \sum_{\mathbf{k} \in \text{sBZ}} (f_A^\dagger(\mathbf{k}), f_B^\dagger(\mathbf{k}), f_A(-\mathbf{k}), f_B(-\mathbf{k})) \times H(\mathbf{k}) \begin{pmatrix} f_A(\mathbf{k}) \\ f_B(\mathbf{k}) \\ f_A^\dagger(-\mathbf{k}) \\ f_B^\dagger(-\mathbf{k}) \end{pmatrix}, \quad (\text{C15})$$

where sBZ is a smaller rectangular BZ with half area. $H(\mathbf{k})$ is

$$H(\mathbf{k}) = \begin{pmatrix} -\mu I & P(\mathbf{k})^\dagger \\ P(\mathbf{k}) & \mu I \end{pmatrix}, \quad (\text{C16})$$

where I is the identity matrix with 2×2 dimension. $P(\mathbf{k})$ is

$$P(\mathbf{k}) = 2i\Delta(\sin k_1 \delta_z + \sin k_2 \sigma_x - \cos k_3 \sigma_y), \quad (\text{C17})$$

where $k_1 = \mathbf{k} \cdot \mathbf{a}_2 = k_x$, $k_2 = \mathbf{k} \cdot \mathbf{a}_2 = -\frac{1}{2}k_x + \frac{\sqrt{3}}{2}k_y$, and $k_3 = \mathbf{k} \cdot (\mathbf{a}_1 + \mathbf{a}_2) = \frac{1}{2}k_x + \frac{\sqrt{3}}{2}k_y$. The dispersion is

$$E(\mathbf{k}) = \sqrt{\mu^2 + 4\Delta^2(\sin^2 k_1 + \sin^2 k_2 + \cos^2 k_3)}. \quad (\text{C18})$$

Self-consistently we find $\Delta = 4.213J$ with mean field energy $E_M = -0.0226 \times 42J$. $\mu = -8.93J$.

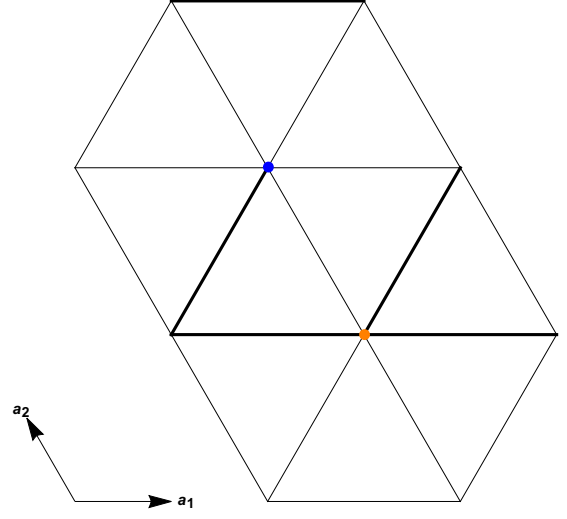


FIG. 6. π -flux Ansatz for Schwinger boson with nearest-neighbor pairing. The pairing term is even under inversion. The bold bond denotes positive pairing while the weak bond denotes negative pairing. There are two inequivalent sublattices.

2. Type II Z_2 spin liquid

The type II Z_2 spin liquid has PSG $P^b = (1, 1, 1)$ and $P^f = (0, 0, 1)$. The bosonic e spinon is in a π -flux phase while the f particle is in a zero-flux phase. We can get the dispersions of the e particle and the f particle from the Schwinger boson and the Schwinger fermion mean field theories, respectively.

a. Mean Field theory of e particle

In the π -flux state, the unit cell is doubled. We have two sublattices A and B . There is only pairing term with pattern shown in Fig. 6. The Hamiltonian is

$$H = \frac{1}{2} \sum_{\mathbf{k} \in \text{sBZ}} (b_A^\dagger(\mathbf{k}), b_B^\dagger(\mathbf{k}), b_A(-\mathbf{k}), b_B(-\mathbf{k})) \times H(\mathbf{k}) \begin{pmatrix} b_A(\mathbf{k}) \\ b_B(\mathbf{k}) \\ b_A^\dagger(-\mathbf{k}) \\ b_B^\dagger(-\mathbf{k}) \end{pmatrix}, \quad (\text{C19})$$

where sBZ is a smaller rectangular BZ with half area. $H(\mathbf{k})$ is

$$H(\mathbf{k}) = \begin{pmatrix} -\mu I & P(\mathbf{k}) \\ P(\mathbf{k})^\dagger & -\mu I \end{pmatrix}, \quad (\text{C20})$$

where I is the identity matrix with 2×2 dimension. $P(\mathbf{k})$ is

$$P(\mathbf{k}) = 2\Delta(\cos k_1 \delta_z + \cos k_2 \sigma_x + \sin k_3 \sigma_y), \quad (\text{C21})$$

where $k_1 = \mathbf{k} \cdot \mathbf{a}_2 = k_x$, $k_2 = \mathbf{k} \cdot \mathbf{a}_2 = -\frac{1}{2}k_x + \frac{\sqrt{3}}{2}k_y$, and $k_3 = \mathbf{k} \cdot (\mathbf{a}_2 - \mathbf{a}_1) = \frac{1}{2}k_x + \frac{\sqrt{3}}{2}k_y$. The energy spectrum is

$$E_{\mathbf{k}} = \sqrt{\mu^2 - 4\Delta^2(\cos^2 k_1 + \cos^2 k_3 + \sin^2 k_2)}. \quad (\text{C22})$$

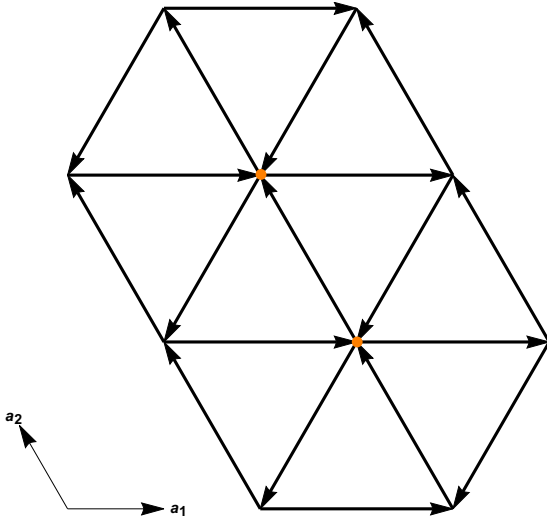


FIG. 7. Zero-flux *Ansatz* for Schwinger fermion with nearest-neighbor pairing. The pairing term is odd under inversion. The direction of the arrow denotes the positive pairing.

The self-consistent equations are

$$\frac{1}{2} \sum_{\mathbf{k} \in \text{sBZ}} \left(\frac{|\mu|}{E_{\mathbf{k}}} - 1 \right) = \frac{1}{6},$$

$$28J \sum_{\mathbf{k} \in \text{sBZ}} \frac{4\Delta(\cos^2 k_1 + \cos^2 k_3 + \sin^2 k_2)}{12E_{\mathbf{k}}} = \Delta. \quad (\text{C23})$$

The sBZ is defined as $k_x \in [-\pi, \pi]$ and $k_y \in [-\frac{\pi}{\sqrt{3}}, \frac{\pi}{\sqrt{3}}]$. The solution is $\Delta = 5.1095J$ with mean field energy $E_{\text{MF}} = -0.0333 \times 42J$. The critical density for condensation is around 5.09, which is quite large.

The band minima of the dispersion are at the following four points: $\mathbf{K}_1 = (\frac{\pi}{6}, \frac{\pi}{2\sqrt{3}})$, $\mathbf{K}_2 = (\frac{5\pi}{6}, \frac{\pi}{2\sqrt{3}})$, $-\mathbf{K}_1$, and $-\mathbf{K}_2$. Condensation of e particle can therefore lead to antiferromagnetic order. Two-spinon spectrum minima: $\mathbf{Q}_1 = \mathbf{K}_2 - \mathbf{K}_1 =$

$(\frac{2\pi}{3}, 0)$, $\mathbf{Q}_2 = \mathbf{K}_1 - (-\mathbf{K}_1) = (\frac{\pi}{3}, \frac{\pi}{\sqrt{3}})$, $\mathbf{Q}_3 = \mathbf{K}_2 - (-\mathbf{K}_2) = (-\frac{\pi}{3}, \frac{\pi}{\sqrt{3}})$, $\mathbf{Q}_4 = \mathbf{K}_1 - \mathbf{K}_2 = (-\frac{2\pi}{3}, 0)$, $\mathbf{Q}_5 = (-\mathbf{K}_1) - \mathbf{K}_1 = (-\frac{\pi}{3}, -\frac{\pi}{\sqrt{3}})$, and $\mathbf{Q}_6 = (-\mathbf{K}_2) - \mathbf{K}_2 = (\frac{\pi}{3}, -\frac{\pi}{\sqrt{3}})$. These six vectors form another hexagon. The enlarged unit cell is $2\sqrt{3} \times 2\sqrt{3}$.

b. Mean field theory of f particle

The PSG for the f particle is $P^f = (0, 0, 1)$. The hopping term is equal for every bond. The pairing term follows the pattern shown in Fig. 7.

The mean field *Ansatz* is

$$H_M = -\mu \sum_i f_i^\dagger f_i - t \sum_{\langle ij \rangle} (f_i^\dagger f_j + \text{H.c.}) - \sum_{\langle ij \rangle} (\Delta_{ij}^* f_i f_j + \text{H.c.}). \quad (\text{C24})$$

We need to fix the filling $\langle f_i^\dagger f_i \rangle = \frac{1}{6}$. The pairing *Ansatz* is $\Delta_{ij} = -\Delta_{ji}$ with $|\Delta_{ij}| = \Delta$:

$$H = \frac{1}{2} \sum_{\mathbf{k} \in \text{BZ}} (f^\dagger(\mathbf{k}), f(-\mathbf{k})) H(\mathbf{k}) \begin{pmatrix} f(\mathbf{k}) \\ f^\dagger(-\mathbf{k}) \end{pmatrix} \quad (\text{C25})$$

with

$$H(\mathbf{k}) = \begin{pmatrix} \xi(\mathbf{k}) & \Delta(\mathbf{k})^* \\ \Delta^\dagger(\mathbf{k}) & -\xi(-\mathbf{k}) \end{pmatrix}. \quad (\text{C26})$$

Let us define $k_1 = \mathbf{k} \cdot \mathbf{a}_1 = k_x$, $k_2 = \mathbf{k} \cdot \mathbf{a}_2 = -\frac{1}{2}k_x + \frac{\sqrt{3}}{2}k_y$, and $k_3 = \mathbf{k} \cdot (\mathbf{a}_1 + \mathbf{a}_2) = \frac{1}{2}k_x + \frac{\sqrt{3}}{2}k_y$. We have

$$\epsilon(\mathbf{k}) = -2t(\cos k_1 + \cos k_2 + \cos k_3), \quad (\text{C27})$$

$$\Delta(\mathbf{k}) = 2i\Delta(\sin k_1 + \sin k_2 - \sin k_3). \quad (\text{C28})$$

The dispersion is

$$E(\mathbf{k}) = \sqrt{[\epsilon(\mathbf{k}) - \mu]^2 + 4\Delta^2(\sin k_1 + \sin k_2 - \sin k_3)^2}. \quad (\text{C29})$$

Self-consistently we find $\Delta = 3.7522J$ with mean field energy $E_M = -0.02039 \times 42J$. $\mu = -7.095J$.

- [1] Y. Cao, V. Fatemi, A. Demir, S. Fang, S. L. Tomarken, J. Y. Luo, J. D. Sanchez-Yamagishi, K. Watanabe, T. Taniguchi, E. Kaxiras *et al.*, *Nature (London)* **556**, 80 (2018).
- [2] Y. Cao, V. Fatemi, S. Fang, K. Watanabe, T. Taniguchi, E. Kaxiras, and P. Jarillo-Herrero, *Nature (London)* **556**, 43 (2018).
- [3] M. Yankowitz, S. Chen, H. Polshyn, Y. Zhang, K. Watanabe, T. Taniguchi, D. Graf, A. F. Young, and C. R. Dean, *Science* **363**, 1059 (2019).
- [4] X. Lu, P. Stepanov, W. Yang, M. Xie, M. A. Aamir, I. Das, C. Urgell, K. Watanabe, T. Taniguchi, G. Zhang *et al.*, *Nature* **574**, 653 (2019).
- [5] A. L. Sharpe, E. J. Fox, A. W. Barnard, J. Finney, K. Watanabe, T. Taniguchi, M. A. Kastner, and D. Goldhaber-Gordon, *Science* **365**, 605 (2019).
- [6] C. Shen, N. Li, S. Wang, Y. Zhao, J. Tang, J. Liu, J. Tian, Y. Chu, K. Watanabe, T. Taniguchi, R. Yang, Z. Y. Meng, D. Shi, and G. Zhang, *arXiv:1903.06952*.
- [7] X. Liu, Z. Hao, E. Khalaf, J. Y. Lee, K. Watanabe, T. Taniguchi, A. Vishwanath, and P. Kim, *arXiv:1903.08130*.
- [8] Y. Cao, D. Rodan-Legrain, O. Rubies-Bigordà, J. M. Park, K. Watanabe, T. Taniguchi, and P. Jarillo-Herrero, *arXiv:1903.08596*.
- [9] G. Chen, L. Jiang, S. Wu, B. Lyu, H. Li, B. L. Chittari, K. Watanabe, T. Taniguchi, Z. Shi, J. Jung, Y. Zhang, and F. Wang, *Nat. Phys.* **15**, 237 (2019).
- [10] G. Chen, A. L. Sharpe, P. Gallagher, I. T. Rosen, E. J. Fox, L. Jiang, B. Lyu, H. Li, K. Watanabe, T. Taniguchi, J. Jung, Z. Shi, D. Goldhaber-Gordon, Y. Zhang, and F. Wang, *Nature* **572**, 215 (2019).

- [11] G. Chen, A. L. Sharpe, E. J. Fox, Y.-H. Zhang, S. Wang, L. Jiang, B. Lyu, H. Li, K. Watanabe, T. Taniguchi *et al.*, [arXiv:1905.06535](#).
- [12] Y.-H. Zhang, D. Mao, Y. Cao, P. Jarillo-Herrero, and T. Senthil, *Phys. Rev. B* **99**, 075127 (2019).
- [13] B. L. Chittari, G. Chen, Y. Zhang, F. Wang, and J. Jung, *Phys. Rev. Lett.* **122**, 016401 (2019).
- [14] Y.-H. Zhang, D. Mao, and T. Senthil, *Phys. Rev. Res.* **1**, 033126 (2019).
- [15] N. Bultinck, S. Chatterjee, and M. P. Zaletel, [arXiv:1901.08110](#).
- [16] N. R. Chebrolu, B. L. Chittari, and J. Jung, *Phys. Rev. B* **99**, 235417 (2019).
- [17] Y. W. Choi and H. J. Choi, *Phys. Rev. B* **100**, 201402(R) (2019).
- [18] J. Y. Lee, E. Khalaf, S. Liu, X. Liu, Z. Hao, P. Kim, and A. Vishwanath, *Nat. Commun.* **10**, 5333 (2019).
- [19] M. Koshino, *Phys. Rev. B* **99**, 235406 (2019).
- [20] J. Liu, Z. Ma, J. Gao, and X. Dai, *Phys. Rev. X* **9**, 031021 (2019).
- [21] H. C. Po, L. Zou, A. Vishwanath, and T. Senthil, *Phys. Rev. X* **8**, 031089 (2018).
- [22] Y.-H. Zhang and T. Senthil, *Phys. Rev. B* **99**, 205150 (2019).
- [23] C. Xu and L. Balents, *Phys. Rev. Lett.* **121**, 087001 (2018).
- [24] G.-Y. Zhu, T. Xiang, and G.-M. Zhang, [arXiv:1806.07535](#).
- [25] C.-M. Jian and C. Xu, [arXiv:1810.03610](#).
- [26] C. Schrade and L. Fu, *Phys. Rev. B* **100**, 035413 (2019).
- [27] F. Wu, T. Lovorn, E. Tutuc, I. Martin, and A. H. MacDonald, *Phys. Rev. Lett.* **122**, 086402 (2019).
- [28] S. E. Sebastian, N. Harrison, M. Altarawneh, C. Mielke, R. Liang, D. Bonn, and G. Lonzarich, *Proc. Natl. Acad. Sci. USA* **107**, 6175 (2010).
- [29] S. Badoux, W. Tabis, F. Laliberté, G. Grissonnanche, B. Vignolle, D. Vignolles, J. Béard, D. Bonn, W. Hardy, R. Liang *et al.*, *Nature (London)* **531**, 210 (2016).
- [30] N. Harrison and S. E. Sebastian, *Phys. Rev. Lett.* **106**, 226402 (2011).
- [31] S. E. Sebastian, N. Harrison, and G. G. Lonzarich, *Rep. Prog. Phys.* **75**, 102501 (2012).
- [32] T. Senthil, S. Sachdev, and M. Vojta, *Phys. Rev. Lett.* **90**, 216403 (2003).
- [33] S. Sachdev and D. Chowdhury, *Prog. Theor. Exp. Phys.* **2016**, 12C102 (2016).
- [34] R. Nandkishore, M. A. Metlitski, and T. Senthil, *Phys. Rev. B* **86**, 045128 (2012).
- [35] J. Thomson, S. Chatterjee, S. Sachdev, and M. S. Scheurer, *Phys. Rev. B* **98**, 075109 (2018).
- [36] J. F. Dodaro, S. A. Kivelson, Y. Schattner, X.-Q. Sun, and C. Wang, *Phys. Rev. B* **98**, 075154 (2018).
- [37] P. A. Lee, N. Nagaosa, and X.-G. Wen, *Rev. Mod. Phys.* **78**, 17 (2006).
- [38] Y.-H. Zhang and A. Vishwanath, [arXiv:1909.12865](#).
- [39] D. Li, K. Lee, B. Y. Wang, M. Osada, S. Crossley, H. R. Lee, Y. Cui, Y. Hikita, and H. Y. Hwang, *Nature (London)* **572**, 624 (2019).
- [40] M. Oshikawa, *Phys. Rev. Lett.* **84**, 3370 (2000).
- [41] T. Senthil, *Phys. Rev. B* **78**, 045109 (2008).
- [42] F. Wang and A. Vishwanath, *Phys. Rev. B* **74**, 174423 (2006).
- [43] A. M. Essin and M. Hermele, *Phys. Rev. B* **87**, 104406 (2013).
- [44] Y.-M. Lu, G. Y. Cho, and A. Vishwanath, *Phys. Rev. B* **96**, 205150 (2017).
- [45] Y. Qi and L. Fu, *Phys. Rev. B* **91**, 100401(R) (2015).
- [46] M. Hermele and X. Chen, *Phys. Rev. X* **6**, 041006 (2016).
- [47] L. B. Ioffe and A. I. Larkin, *Phys. Rev. B* **39**, 8988 (1989).
- [48] Y.-Z. You, Y.-C. He, C. Xu, and A. Vishwanath, *Phys. Rev. X* **8**, 011026 (2018).